

AD 748098



AD

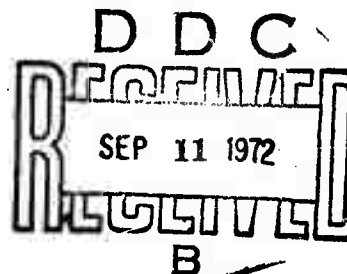
SEE AD 737276

AMMRC CR 71-2/4

THE EFFECTS OF SURFACE LAYER ON PLASTIC DEFORMATION
AND CRACK PROPAGATION

July 1972

I. R. Kramer, A. Kumar, and N. Balasubramanian
Martin Marietta Corporation, Denver Division
P. O. Box 179, Denver, Colorado 80201



Semiannual Report

Contract DAAG 46-70-C-0102

Approved for public release; distribution unlimited

Prepared for

Reproduced by
NATIONAL TECHNICAL
INFORMATION SERVICE
U S Department of Commerce
Springfield VA 22151

ARMY MATERIALS AND MECHANICS RESEARCH CENTER
Watertown, Massachusetts 02172

**BEST
AVAILABLE COPY**

ACCESSION for		
NTIS	White Section	<input checked="" type="checkbox"/>
DDC	Black Section	<input type="checkbox"/>
UNAL CHANGED		<input type="checkbox"/>
JUSTIFICATION		
BY		
DISTRIBUTION/AVAILABILITY CODES		
Dist.	A,AIL and/or SPECIAL	
A		

The findings in this report are not to be construed as an official Department of the Army position, unless so designated by other authorized documents.

Mention of any trade names or manufacturers in this report shall not be construed as advertising nor as an official indorsement or approval of such products or companies by the United States Government.

DISPOSITION INSTRUCTIONS

Destroy this report when it is no longer needed.
Do not return it to the originator.

DOCUMENT CONTROL DATA - R & D

(Security classification of title, body of abstract and indexing annotation must be entered when the overall report is classified)

1. ORIGINATING ACTIVITY (Corporate author)

Martin Marietta Corporation

2a. REPORT SECURITY CLASSIFICATION

Unclassified

2b. GROUP

3. REPORT TITLE

The Effects of Surface Layer on Plastic Deformation and Crack Propagation

4. DESCRIPTIVE NOTES (Type of report and inclusive dates)

Semiannual Report, January 1972 to July 1972

5. AUTHOR(S) (First name, middle initial, last name)

I. R. Kramer and A. Kumar

6. REPORT DATE

July 1972

7a. TOTAL NO. OF PAGES

79

7b. NO. OF REFS

15

8a. CONTRACT OR GRANT NO.

DAAG 46-70-C-0102

b. PROJECT NO.

ARPA Order 1576

c.

d.

9a. ORIGINATOR'S REPORT NUMBER(S)

AMMRC CR 71-2/4

9b. OTHER REPORT NO(S) (Any other numbers that may be assigned this report)

10. DISTRIBUTION STATEMENT

Approved for public release; distribution unlimited.

11. SUPPLEMENTARY NOTES

12. SPONSORING MILITARY ACTIVITY

Army Materials and Mechanics Research Cent
Watertown, Massachusetts 02172

13. ABSTRACT

In Chapter I, metallographic evidence of the existence of the surface layer is given. Using etch-pit techniques on an iron-silicon alloy, it is shown that the dislocation concentration of strained specimens decreases away from the surface. In Chapter II, a relationship is given between the surface-layer stress and fatigue failure. When surface-layer stress attains a critical value, the specimens fractured. An excellent correlation is reported between the life predicted from surface-layer stress data and fatigue life found experimentally. In Chapter III, surface-layer stress at the root of notches is reported. The surface-layer stress was found to increase rapidly as the stress concentration increased. In Chapter IV, the crack propagation rate for an iron-silicon alloy is reported. The crack propagation rate under plane stress conditions decreased in specimens given the SLE treatment. An examination of the surfaces showed that the dislocation concentration was much lower in the SLE-treated sample than in the untreated specimens. Chapter V reports an unsuccessful attempt to detect slip-line formation and strain under sustained loads up to 500 hr. It is believed that greater measurement sensitivity is required for successful detection.

KEY WORDS

Crack Propagation
Stress Intensity
Crack Growth
Surface Layer
Fatigue

LINK A

LINK B

LINK C

ROLE

WT

ROLE

WT

ROLE

WT

AMMRC CR 71-2/4

THE EFFECTS OF SURFACE LAYER ON PLASTIC DEFORMATION
AND CRACK PROPAGATION

July 1972

I. R. Kramer, A. Kumar, and N. Balasubramanian
Martin Marietta Corporation
P. O. Box 179, Denver, Colorado 80201

Semiannual Report

Contract DAAG 45-70-C-0102

Approved for public release; distribution unlimited

FOREWORD

This report was prepared by the Denver Division of Martin Marietta Aerospace under U. S. Army Contract DAAG 46-70-C-0102. The contract is sponsored by the Advanced Research Project Agency under ARPA Order 188-0-7400 and is being administered by the Army Materials and Mechanics Research Center, Watertown, Massachusetts, with Dr. Eric B. Kula, AMXMR-EM, serving as Technical Supervisor.

This report has been divided into five chapters. Each chapter has been written as a complete entity, independent from the others.

- Chapter I. Metallographic Study of the Surface Layer
- II. A Mechanism of Fatigue Failure
- III. Surface-Layer Stress at Notches
- IV. Crack Propagation in an Iron-Silicon Alloy
- V. Deformation under Sustained Load

ABSTRACT

In Chapter I, metallographic evidence of the existence of the surface layer is given. Using etch-pit techniques on an iron-silicon alloy, it is shown that the dislocation concentration of strained specimens decreases away from the surface. In Chapter II, a relationship is given between the surface-layer stress and fatigue failure. When surface-layer stress attains a critical value, the specimens fractured. An excellent correlation is reported between the life predicted from surface-layer stress data and fatigue life found experimentally. In Chapter III, surface-layer stress at the root of notches is reported. The surface-layer stress was found to increase rapidly as the stress concentration increased. In Chapter IV, the crack propagation rate for an iron-silicon alloy is reported. The crack propagation rate under plane stress conditions decreased in specimens given the SLE treatment. An examination of the surfaces showed that the dislocation concentration was much lower in the SLE-treated sample than in the untreated specimens. Chapter V reports an unsuccessful attempt to detect slip-line formation and strain under sustained loads up to 500 hr. It is believed that greater measurement sensitivity is required for successful detection.

CONTENTS

	<u>Page</u>
I. Metallographic Study of Surface Layer	
Introduction	I-1
Experimental	I-5
Results and Discussion	I-6
Summary	I-17
Acknowledgment	I-17
Bibliography	I-18
II. A Mechanism of Fatigue Failure	
Introduction	II-1
Experimental	II-4
Results and Discussion	II-5
Summary	II-19
References	II-22
III. Surface-Layer Stress at Notches	
Introduction	III-1
Experimental Procedure	III-2
Results	III-2
References	III-7
IV. Crack Propagation in Iron-Silicon Alloy	
Introduction	IV-1
Experimental Techniques	IV-2
Results and Discussion	IV-6
References	IV-12
V. Deformation under Sustained Load	
Introduction	V-1
Experimental Techniques	V-2
Results and Discussion	V-6
References	V-7

Fig. I-1	Typical Changes in Dislocation Etch-Pit Density for a given area as a Function of Depth, Δx , from the Surface of a Strained Fe-3% Si Alloy	I-7
Fig. I-2	Dislocation Density, p , as a Function of Depth, Δx , from the Surface in Fe-3% Si Alloy	I-9
Fig. I-3	The Threshold Stress, σ_{th} , for Plastic Flow of Aluminum monocrystals Strained 5% as a Function of Depth, Δx , from the Surface . .	I-10
Fig. I-4	The Threshold Stress, σ_{th} , for Plastic Flow of 2014-T6 Stressed to 42 kg/mm ² as a Function of Depth, Δx , from the Surface . .	I-12
Fig. I-5	Percentage of Surface grains Deformed as a Function of Applied Stress, σ , in 2014-T6	I-13
Fig. I-6	The Threshold Stress, σ_{th} , for Plastic Flow of Fe-3% Si Alloy Strained 1% as a Function of Depth, Δx , from the Surface; Metallographic Data-0, Stress-Strain Data-X	I-14
Fig. I-7	Correlation between Surface Layer Stress, σ_s , and the Excess Dislocation Density in Surface Layer, ρ_s , for Fe-3% Si Alloy Strained 1%, $\dot{\epsilon} = 2 \times 10^{-5}$ /sec	I-16
Fig. II-1	Schematic Representation of Surface Layer	II-3
Fig. II-2	Typical Load-Deformation Curve	II-6
Fig. II-3	Increase in Surface-Layer Stress in 6AL/4V with Number of Fatigue Cycles and Stress Amplitude, $R = -1$	II-8

Fig. II-4	Increase in Surface Layer Stress in 2014-T6 with Number of Fatigue Cycles and Stress Amplitude, $R = -1$	II-9
Fig. II-5	Increase in 6Al/4V Fatigue Life by Re- moval of Surface Layer, $R = -1$	II-11
Fig. II-6	Increase in 2014-T6 Fatigue Life by Re- moval of Surface Layer, $R = -1$	II-12
Fig. II-7	Relationship between Slope $S = d\sigma_s/dN$ and Stress Amplitude	II-14
Fig. II-8	Relationship between Fatigue Life and Stress Amplitude	II-16
Fig. II-9	Crack Propagation Behavior of 2014-T6 under Plane Strain Conditions, Compact Tension Specimens 1-in. Thick	II-17
Fig. II-10	Crack Propagation Behavior of 2014-T6 under Plane Strain Conditions, Compact Tension Specimens 1-in. Thick	II-20
Fig. II-11	Crack Propagation Behavior of 6Al/4V under Plane Stress Conditions Center- Cracked Specimens 0.067-in. Thick	II-21
Fig. III-1	Configuration of Creep Specimen	III-3
Fig. III-2	Effect of Notches on Surface-Layer Stress of 6Al/4V	III-4
Fig. III-3	Relaxation of Surface-Layer Stress of 60° Notched Specimens of 6Al/4V, $R = -1$	III-6
Fig. IV-1	Voltage-Current Density Curve for Electro- lytic Etching of Fe-3% Si	IV-3
Fig. IV-2	Center-Cracked Plane Stress Specimen Configuration	IV-5

Fig. IV-3	Fe-3% Si, Cyclic Crack Propagation Behavior, plane Stress Condition	IV-7
Fig. IV-4	Fe-3% Si Crack growth Rate, Plane Stress Condition	IV-9
Fig. IV-5	Dislocation Density as a Function of Depth, Δx , in Vicinity of Crack in Untreated (a,b,c) and SLE Treated (d,e,f) Fe-3% Si	IV-11
Fig. V-1	Center-Cracked Specimen Configuration . . .	V-4
Fig. V-2	Proportions of Modified Compact Tension Specimen	V-5
Fig. V-3	Branched Crack Formed during Application of Load on CTS Specimen of 2014-T6, 75X	V-7

TABLE

II-1	Extension of Fatigue Life by Removal of Surface Layer	II-10
------	--	-------

I. Metallographic Study of the Surface Layer

INTRODUCTION

Based on observations that the slope and extent of Stages I and II of the stress-strain curve were markedly affected when f.c.c. crystals were deformed while metal was being removed, Kramer (1963) advanced the idea that work hardening was not uniform throughout the cross-section of a specimen pulled in uniaxial tension.

In those experiments it was shown that the slopes decreased and the extent of Stages I and II increased with the rate of metal removal. From this it was also concluded that the conditions at the surface were such that a back stress existed which opposed the motion of dislocations in the interior. Later, Kramer (1965) showed that when a specimen was deformed to a given strain and then unloaded, upon reloading after removal of a given amount of metal, the initial flow stress, as measured by the departure from linearity of the stress-strain curve, was lower than that to which the specimen had been strained. This difference, $\Delta\sigma$, between the two stresses increased with the amount of metal removed until a critical depth was reached and therefore $\Delta\sigma$ remained constant. This difference in stress was defined as the surface layer stress, σ_s . The depth of the surface layer was reported to be about 50 μ for aluminum monocrystals and 100 μ for polycrystalline iron. The concept that a surface layer, harder than the interior, was formed as a result of plastic deformation was further confirmed by measurements of the activation energy and activation volume for plastic deformation.

These measurements (Kramer 1964) showed that the apparent activation energy decreased and the activation volume increased when the surface layer was removed or reduced. Since the activation volume, V^* , is inversely related to the dislocation density and a decrease in activation energy is equal to $V^*\tau^*$, that is $U = U_0 - V^*\tau^*$,

where τ^* is the net stress acting on the dislocations to cause motion, these measurements show the dislocation density in the surface layer is larger than that in the interior of the specimen. Still further evidence for the existence of a hard surface layer may be found in observations concerned with the creep behavior of metals. By removing metal from the surfaces of specimens while they were creeping under constant stress, the creep rate could be increased by a factor of 100 (Kramer 1963). These latter experiments again indicate that the back stress was being reduced by the removal or reduction of the surface layer stress.

In certain metals the surface layer is very unstable and is often completely eliminated by relaxation at room temperature. For example, in high-purity polycrystalline aluminum and copper, the surface layer relaxed completely in 4 and 48 hours, respectively, when specimens 30 mm in diameter were used. This relaxation is accompanied by a change in strain which is opposite to that employed in deforming the specimen. Thus, when a specimen is pulled in tension, after unloading the surface layer is in compression, and when the specimen is compressed, the surface layer is in tension after removal of the load. This indicates that there is an excess number of dislocations of like sign in the surface layer.

From the above it is seen that evidence for the existence of a surface layer which resists plastic deformation is indirect. The data concerned with the extension and slope of Stages I and II, the activation energy and activation volume and measurements of the surface layer stress all demonstrate that the surface layer is "hard", that is it acts to hinder plastic deformation. In all of these investigations, the experiments were conducted by measuring the appropriate change in property after elimination of the surface layer. However, Fourie (1968) attempted to measure the mechanical behavior of specimens taken from the

surface layer. To this end, he strained monocrystals of copper of rectangular cross-sections 2 mm x 10 mm (Fourie 1968) and by jet cutting machined specimens 0.07 mm thick. Unfortunately, no detailed information was given pertaining to the shape of the specimen; the method of measuring strain; and most important, the method of preventing the very thin specimens cut from the surface layer from bending when they were released from the bulk material. As pointed out above, the surface layer would be in a compressive state and a high stress would be imparted to the specimen during the cutting action. Embedding the surface layer specimens in wax during the cutting procedure as done by Fourie (1968) would not prevent bending caused by the difference in stress states between the surface layer and the interior of the strained specimens. Relaxation effects would tend to eliminate the excess dislocations in the surface layer. Nevertheless, Fourie (1968) confirmed existence of the surface layer but reported that the surface layer was "softer" than the bulk material after the specimen was strained. He reported that the surface layer specimens cut from strained large crystals began to flow plastically at a stress lower than that for specimens cut from the bulk. In some cases plastic flow began in the thin surface layer specimens at a stress below that imparted during the prestressing of the large crystal. Size effect considerations would have led to the expectations that the yield and flow strength would increase with decreasing specimen size (Kramer 1967).

Although investigations have been conducted to obtain visual information on the surface layer, the reported results are conflicting. Kitajama, Tanaka, and Kaiede (1969) deformed monocrystals of copper and reported from etch-pit observations that the dislocation density was highest at the surface and decreased with the distance from the surface until a value of about 50 to 100 μ was

reached. Thereafter the dislocation density remained constant. Block and Johnson (1969), ostensibly using the same techniques on copper crystals, reported no change in the dislocation density as a function of distance from the surface. Vellaikal and Washburn (1969) reported that for small strains the surface grains deformed more than grains in the interior and therefore were hardened to a greater extent. Mughrabi (1970), using a thin film electron microscopy technique on copper specimens which had been strained and radiated with neutrons in an attempt to pin the dislocation, reported that the dislocation density in the surface region was lower than that in the interior. It is not possible because of lack of detailed information to reconcile the conflict in the results obtained; however, it is suggested that because of the high relaxation rate of the surface layer, especially in high-purity metals, in some cases surface layer was not present during the observations. However, such dislocation density observations may be made on systems such as precipitation-hardening alloys, where the dislocations in the surface layer are strongly pinned (Kramer 1969) or if the specimens are held at low temperatures. To this end, it was the purpose of this program to investigate the surface layer by metallographic methods. The investigation consisted of (a) measurements by means of etch-pits of the dislocation density as a function of depth from the surface of deformed iron-3% silicon alloy and (b) determination of the onset of plastic flow as a function of depth in strained specimens of monocrystals of aluminum and a polycrystalline 2014-T6 aluminum alloy and iron-3% silicon alloy by the appearance of slip bands.

EXPERIMENTAL

The iron-3% silicon alloy used in this investigation was kindly supplied by A. R. Rosenfield of the Battelle Memorial Institute and was from the same batch of material used successfully in determining the dislocation density in Hahn, Mincer, and Rosenfield (1971). The etchant and procedures were the same as those employed by Hahn, Mincer, and Rosenfield. This material was machined into specimens which were 3.5 mm thick and 70 mm long. The specimens had a reduced gage section 5 mm wide. The grip section of the specimen was 13 mm wide. For the etch-pit determinations, the specimens were first annealed in vacuum at 780°C for four hours and then polished manually to obtain a finish suitable for metallographic examination. Diamond paste of one-micron mesh was used for the final abrasive. The specimens were strained 1 and 1.5 percent in an Instron Tensile Machine. Afterwards, the specimens were aged in vacuum at 150°C for 20 minutes. The etch-pitting was performed as recommended by Hahn, Mincer, and Rosenfield. To obtain measurements of the dislocation density as a function of depth, the specimen was manually polished with diamond paste to the desired depth and care was taken to remove all evidence of previous pits. The specimen was then re-etched under closely controlled conditions to assure that all conditions were duplicated. During the investigation at least five areas along the specimen were studied. The location of these areas was determined by means of marks placed on the gage section and a micrometer stage. A given area could be located within 0.01 mm.

The dislocation density was determined with the aid of a microdensitometer equipped with a recording chart. Each area was traversed completely at least 10 times to obtain a representative average of the dislocation density of the region under consideration.

To determine the onset of plastic flow as a function of distance, Δx , from the surface of strained specimens, single crystals of aluminum (99.995%), aluminum 2014-T6, and iron-3% silicon were used. The aluminum crystal specimen was 12 mm square in cross-section and 100 mm long while the 2014 aluminum specimens were of the same type as those used in the iron-silicon experiments. The specimens were first stressed to a predetermined value, and a given amount of metal was removed by manually polishing with diamond paste. The aluminum 2014-T6 specimen was stressed to 42 kg/mm² corresponding to a total strain of 0.006 while the monocrystal was stressed to a tensile stress of 0.75 kg/mm², corresponding to a total shear strain of five percent. Again, care was taken to remove all evidence of previously formed slip bands. The specimen was then stressed in an Instron Tensile Machine (200-lb capacity) and the stress required to initiate slip was determined by periodically examining the specimens at a magnification of 1200. This procedure was repeated on the specimen until the stress required to cause slip to be initiated remained constant with the amount of metal removed. A similar series of experiments were conducted on the iron-3% silicon alloy. The specimens were strained one percent (54 kg/mm²) and the stress for the onset of slip was determined as a function depth, Δx , from the surface by noting the appearance of the slip bands.

RESULTS AND DISCUSSION

The photomicrographs in Figure I-1 give visual evidence of the change in dislocation density of the Fe-3% Si alloy strained 1.5% as a function of depth, Δx , from the surface. These results are typical of the other five areas examined. It is very clear that



$\epsilon = 1.5\%$, $\Delta x = 0$



$\epsilon = 1\%$, $\Delta x = 0$



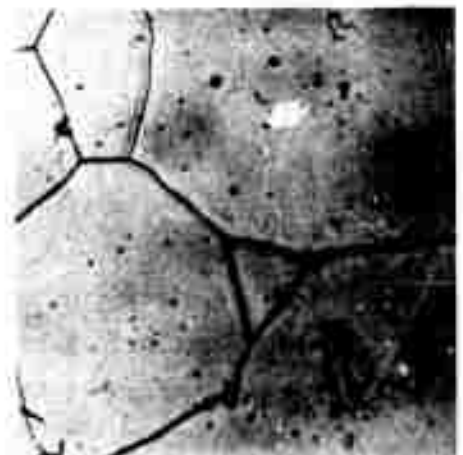
$\epsilon = 1.5\%$, $\Delta x = .075 \text{ mm}$



$\epsilon = 1\%$, $\Delta x = .075 \text{ mm}$



$\epsilon = 1.5\%$, $\Delta x = .138 \text{ mm}$



$\epsilon = 1\%$, $\Delta x = .188 \text{ mm}$

Figure I-1 Typical Changes in Dislocation Etch-Pit Density for a Given Area as a Function of Depth, Δx , from the Surface of a Strained Fe-3% Si Alloy

the dislocation density decreases toward the interior of the specimen. In Figure I-2 the dislocation density is plotted as a function of distance from the surface. Confirming previous results (Kramer 1963), the dislocation density decreases rapidly with the distance from the surface and becomes constant after a depth of about 100 μ . The depth of the surface layer on monocrystals of aluminum and iron as measured by the decrease in initial flow stress after removal of the surface layer was 60 and 100 μ , respectively for 3-mm diameter specimens (Kramer 1963 and 1967). The depth of the surface layer of copper monocrystals was reported to be about 100 μ (Kitajama, Tanaka, and Kaiede 1969). In performing the above investigation a number of observations were made to assure that, during the measurements, no relaxation or loss of dislocation occurred. To this end, iron-3% silicon specimens were strained and aged and then stored for several days. An examination indicated that the dislocation density did not change noticeably during the storage period.

The evidence for the existence of a "hard" surface layer in aluminum monocrystals is presented in Figure I-3. As measured by the first appearance of slip bands, the initial flow stress of crystals which had been strained five percent decreased as a function of depth from the surface up to a distance of about 75 μ . This depth for the surface layer is in close accord with the value of 60 μ measured previously (Kramer 1965). Further, from Figure I-3 the surface layer stress, σ_s , is 196 gr/mm². This value is in good agreement with 155 gr/mm² ($\tau_c = 77.5$ gr/mm²) obtained for 3-mm diameter aluminum crystals (Kramer 1965). It should be noted that during this investigation the specimens were stored when necessary in liquid nitrogen to prevent loss of dislocation by relaxation.

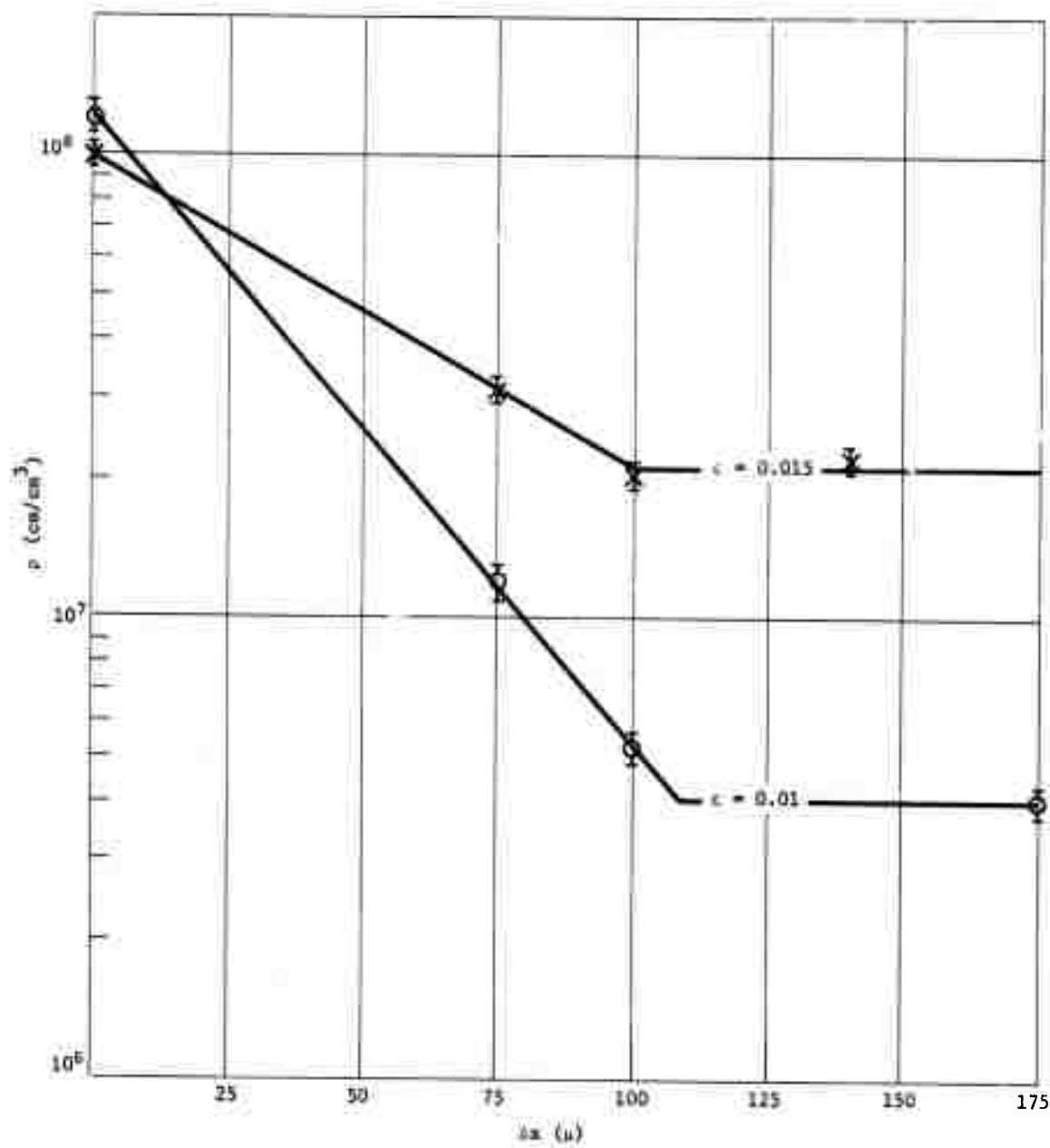


Figure 1-2 Dislocation Density, ρ , as a Function of Depth, Δx from the Surface in Fe-3% Si Alloy

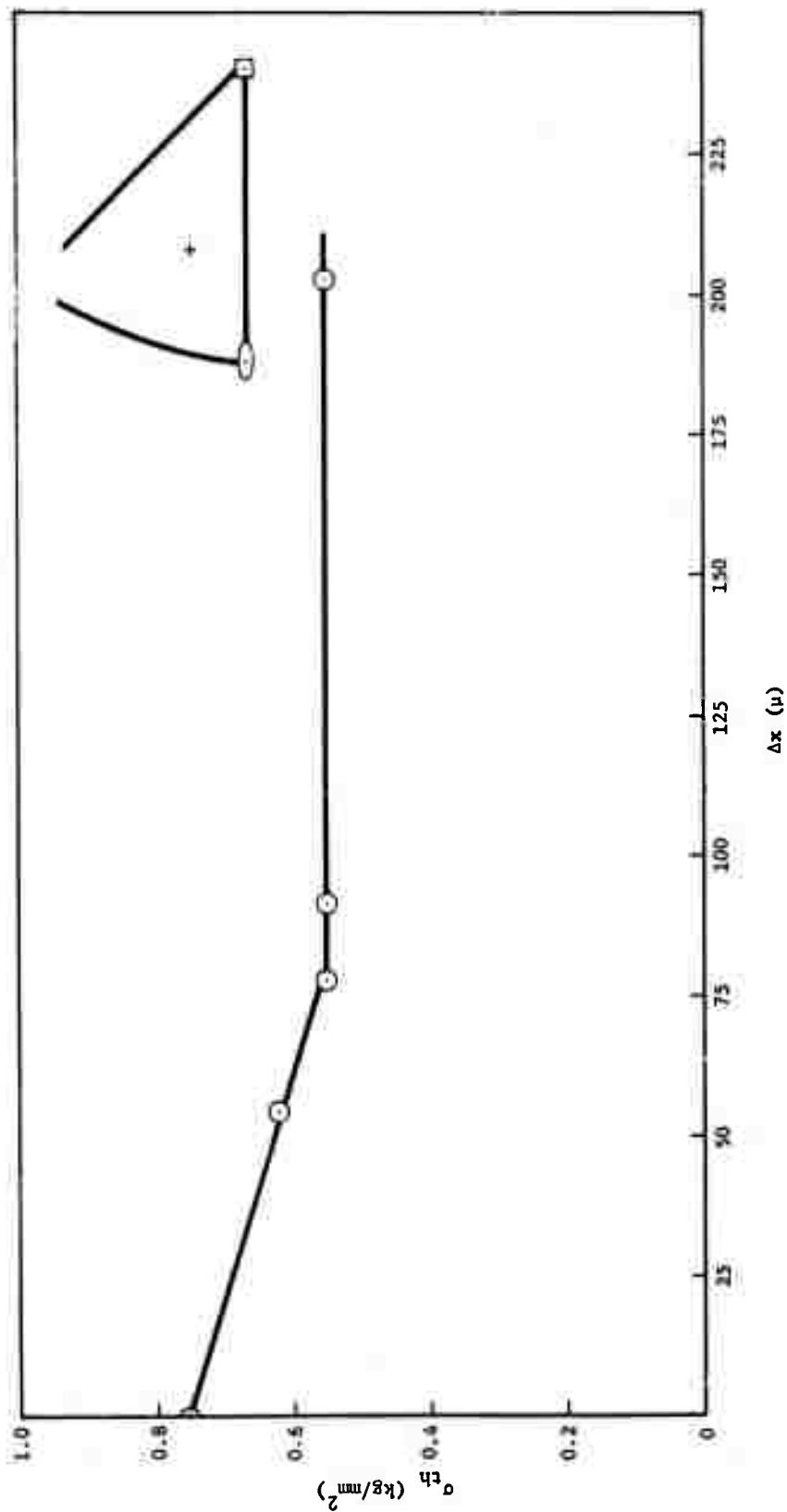


Figure I-3 The Threshold Stress, σ_{th} , for Plastic Flow of Aluminum Monocrystals Strained 5% as a Function of Depth, Δx , from the Surface

The distribution of plastic strain when polycrystalline 2014-T6 aluminum alloy is stressed is given in Figures I-4 and I-5. The data in Figure I-5 give the percentage of surface grains that undergo plastic deformation at various stress levels. These data were obtained by counting the number of grains which contained slip band markings within an area of about 3 cm^2 (1000 grains). For this material the appearance of slip band began at a stress of 3.5 kg/mm^2 . The number of surface grains which deformed plastically thereafter increased very rapidly with stress, and at a stress of 14 kg/mm^2 about 80 percent of the surface grains were deformed. Thereafter, the fraction of surface grains plastically deformed increased slowly and at 0.2 percent of the yield value all of the surface grains deformed.

The preferential hardening of the surface layer for specimens which had been stressed to 42 kg/mm^2 is shown in Figure I-4. At this stress value the stress-strain curve begins to depart from linearity as measured on a scale where 2.5 cm on the chart is equal to 0.0025 cm deflection. As measured by the appearance of slip bands, it is seen that a region 50μ deep has been hardened to a greater extent than the bulk. In these measurements the stress at which about 1% of the grains were deformed was used as the index for the initial plastic deformation. As seen from the slope of the curve in Figure I-5, a difference of one percent of the grains deformed corresponds to a change of only 35 gr/mm^2 . The differential in the work hardening taken as the difference between the peak value of the stress in the hardened surface layer and bulk is about 17.5 kg/mm^2 . In addition, the interior of the specimen was work hardened from 3.5 to 23.8 kg/mm^2 .

The preferential hardening of the surface layer on the iron-3% silicon alloy which had been strained one percent is given in Figure I-6. Similar to that found for the aluminum alloy 2014-T6 and

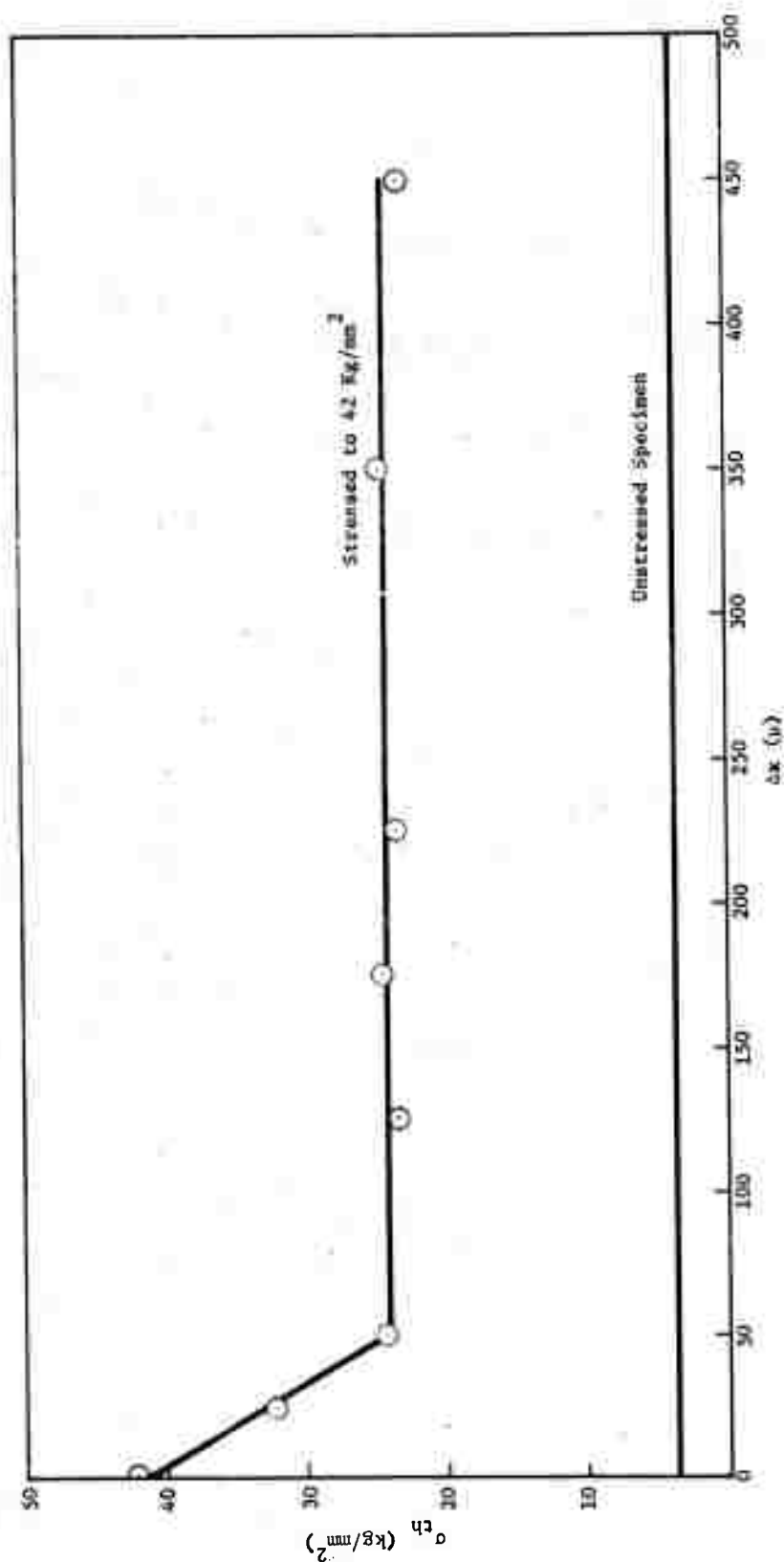


Figure I-4 The Threshold Stress, σ_{th} , for Plastic Flow of Al2014-T6 Stressed to 42 kg/mm^2 as a Function of Depth, Δx , from the Surface

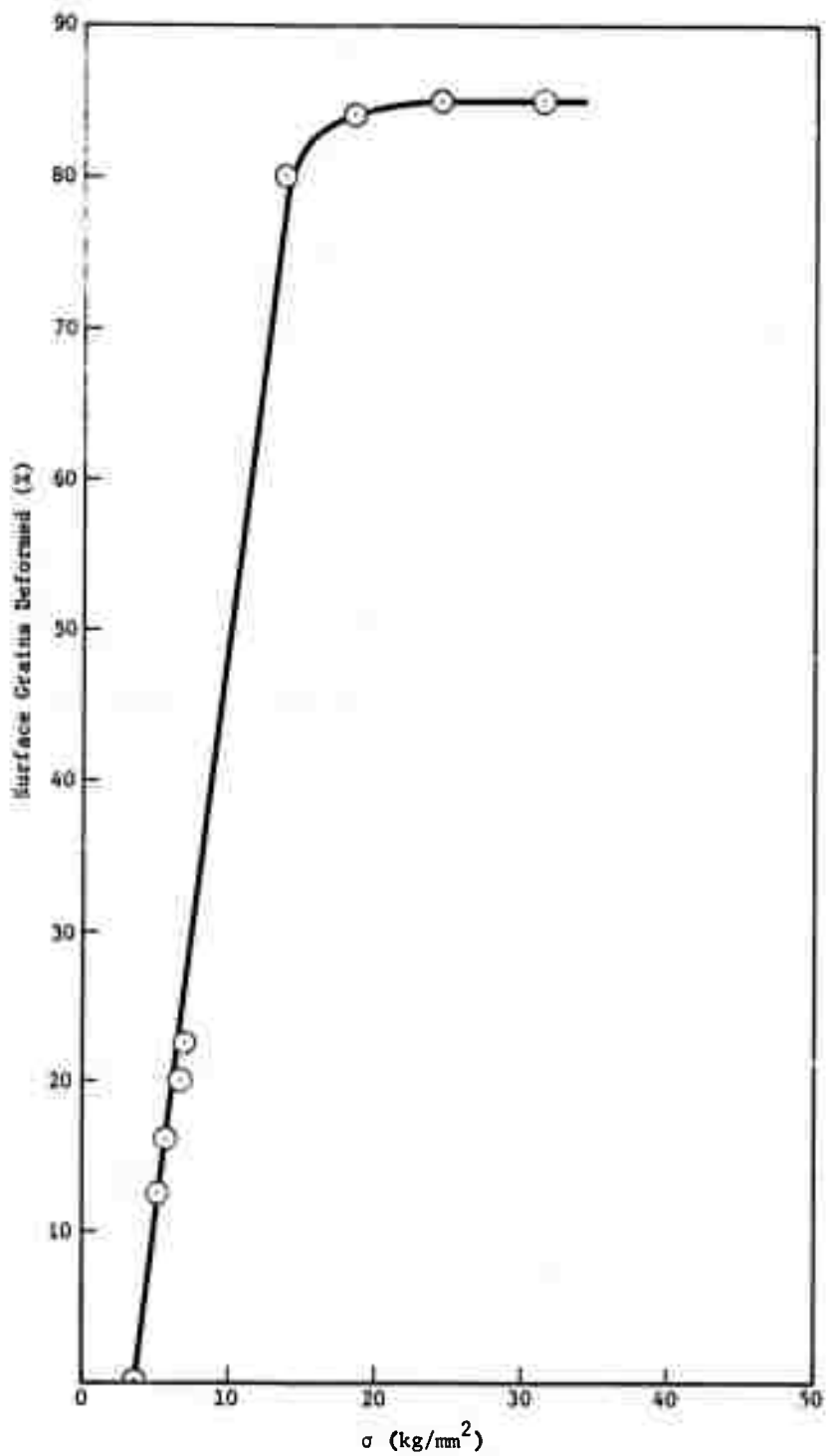


Figure I-5 Percentage of Surface Grains Deformed as a Function of Applied Stress, σ , in Al2014-T6

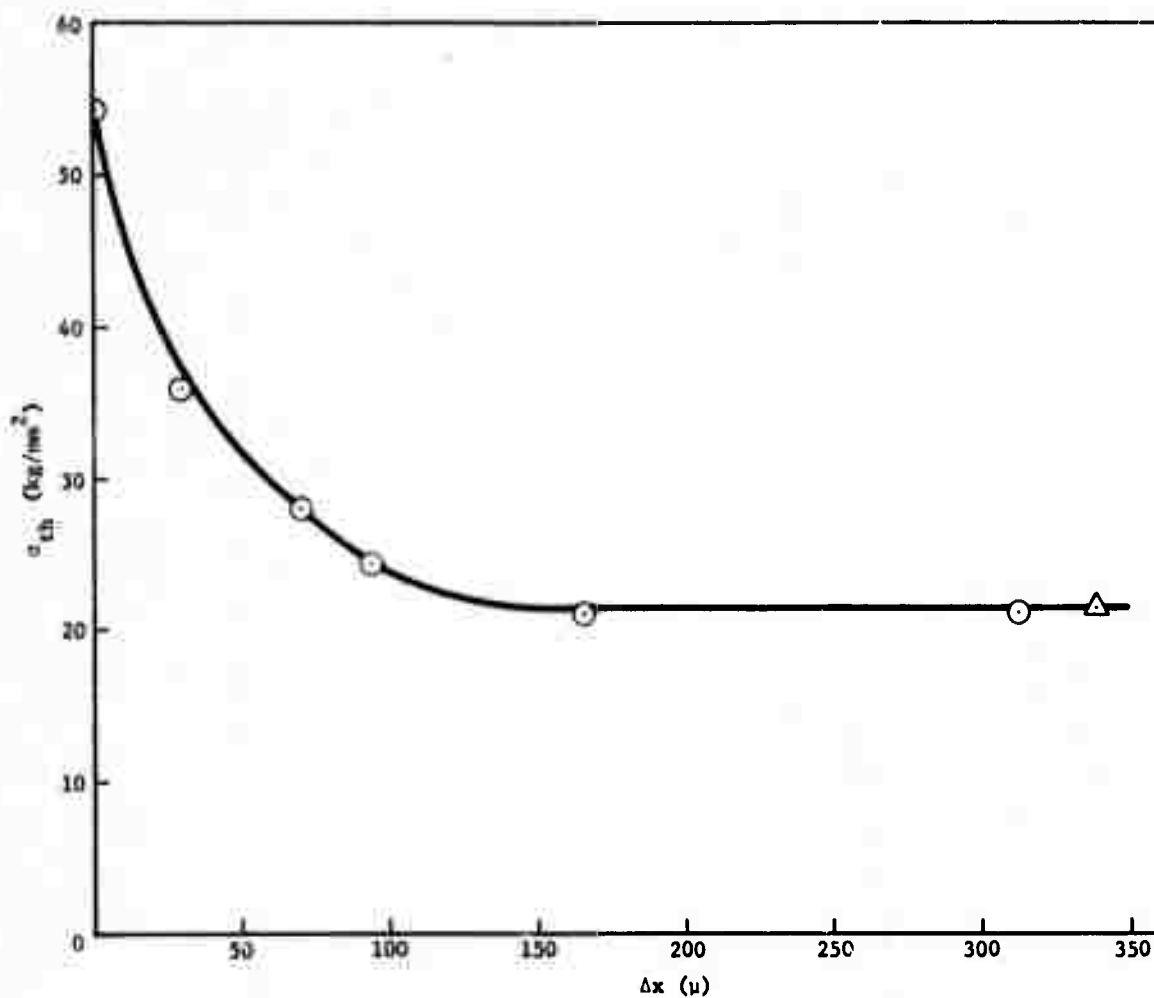


Figure I-6 The Threshold Stress, σ_{th} , for Plastic Flow of Fe-3% Si Alloy Strained 1% as a Function of Depth, Δx , from the Surface; Metallographic Data - \circ , Stress-Strain Data - Δ

the aluminum monocrystals, as measured by the appearance of the slip bands, the work-hardening decreased as a function of depth towards the interior. After a depth between 100 and 150 μ is exceeded, the stress required for the initiation of plastic flow remains constant at a value of 21 kg/mm². The surface layer stress as measured by the difference between the initial stress to attain the one percent strain and the stress required from the initiation of slip bands was 33.3 kg/mm². In an independent experiment the surface layer stress was measured by pulling a specimen to one percent and determining the difference between the unload stress and the stress at which the stress-strain curve departed from linearity after removal of the surface layer. The surface layer stress measured by this method was 32.3 kg/mm².

It was of interest to plot the dislocation density, ρ_s , (Figure I-2) as a function of the surface layer stress, σ_s , (Figure I-6). It should be pointed out that the dislocation density as reported here is given for a selected area while the surface layer stress is given as an average value. Nevertheless when the surface layer stress, σ_s , is plotted as a function of $\rho_s^{1/2}$, a linear relationship is obtained and the curve passes through the origin (Figure I-7). This again shows that the surface layer stress is related to the increase in the dislocation density in the surface layer.

To further supplement the evidence for the preferentially work-hardened surface regions, microhardness measurements were performed on five copper crystals having a square cross-section of 3 mm and which had been strained 1.5%. These measurements were conducted on a microhardness tester using a 35-gram load. With these types of measurements the number of meaningful observations is limited by the depth of penetration of the indenter and therefore an accurate profile of the hardness as a function of depth was not attempted. The measurements showed that after the 1.5%

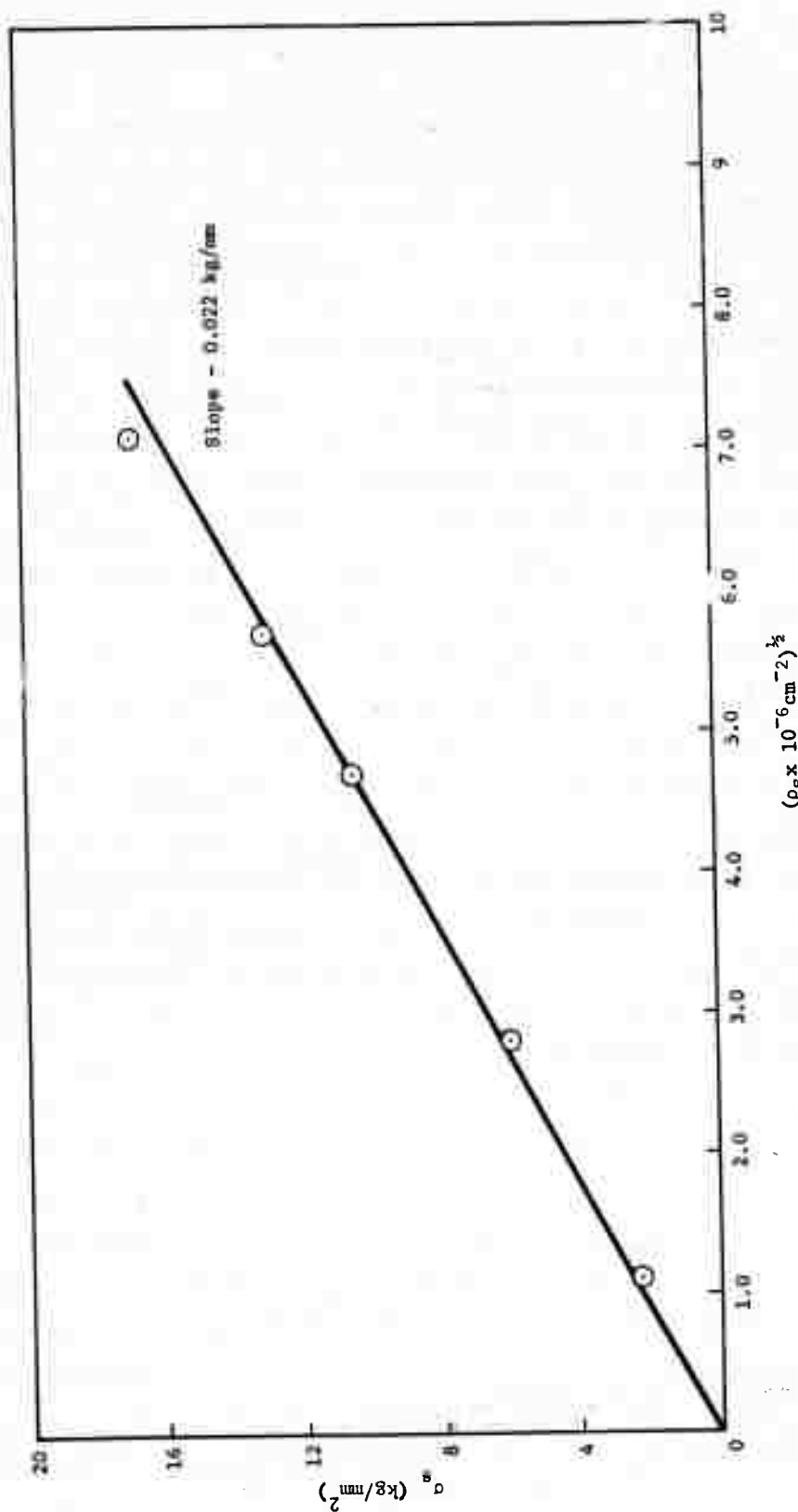


Figure I-7 Correlation between Surface Layer Stress, σ_s , and the Excess Dislocation Density in Surface Layer, ρ_s , for Fe-3% Si Alloy Strained 1%, $\dot{\epsilon} = 2 \times 10^{-5}/\text{sec}$

strain, the Vickers hardness taken on the original surface was 17.3 ± 0.1 . After the specimens were electrochemically polished and 70μ was removed from the surface, the Vickers hardness measurement was 9.6 ± 0.1 . With further removal of metal, the hardness value did not change.

SUMMARY

Measurements of the density of etch pits on iron-3% silicon show that in deformed specimens the dislocation density is highest at the surface and decreases with distance from the surface. At depths greater than 100μ the dislocation density remains constant.

As measured by the stress required for the formation of slip band in aluminum monocrystals and in polycrystalline 2014-T6 aluminum and iron-3% silicon, a work-hardened layer (surface layer) which extends to a depth of 50 to 60μ is formed in plastically strained specimens. Microhardness measurements on copper single crystals also show that strained specimens harden preferentially at the region of the surface.

ACKNOWLEDGMENT

This work was supported in part by the Advanced Research Projects Agency.

BIBLIOGRAPHY

- R. J. Block and R. M. Johnson, 1969, Acta. Met. 17, 1969.
- J. T. Fourie, 1968, Phil. Mag., 17, 735.
- G. Hahn, P. N. Mincer, and A. R. Rosenfield, 1971, Experimental Mechanics. II, 1.
- S. Kitajama, H. Tanaka, and H. Kaiede, 1969, Trans. J.I.M., 10, 1969
- I. R. Kramer, 1964, Trans. AIME, 227, 1003.
- I. R. Kramer, 1964, Trans. AIME 230, 991.
- I. R. Kramer, 1965, Trans. AIME 233, 1462
- I. R. Kramer, *Environment Sensitive Mechanical Behavior*, Gordon and Breech, N.Y., 1965.
- I. R. Kramer, 1967, Trans. AIME 239, 1754.
- I. R. Kramer, 1967, Trans. AIME 239, 520.
- I. R. Kramer, 1970, Proc. Air Force Conf. on Fatigue and Fractures of Aircraft Structures and Materials, AFFDL 70-144.
- H. Mughrabi, 1970, Phys. Stat. Solidi 29, 317.
- G. Vellaikal and J. Washburn, 1969, J. Appl. Phys., 40, 2280.

II. A Mechanism of Fatigue Failure

INTRODUCTION

Previous publications (Ref 1, 2, 3) advanced the concept that the surface layer greatly influences fatigue failures. It was later shown that, during fatigue cycling under either constant strain or constant stress, the surface-layer stress increases (Ref 4). This increase in surface-layer work-hardening is accompanied by a decrease in activation area for plastic flow, and further research showed that the dislocation density in the surface layer increases. In addition, the rate of increase of surface-layer stress with number of fatigue cycles is strongly affected by the environment (Ref 5). In our concept of fatigue failure, it was assumed that, during cycling, the surface layer work-hardens and acts as a barrier to support a piled-up array of dislocations. The effective number of dislocations that the surface layer can support will, of course, depend on the strength of the surface layer. Fatigue cracks will start when the surface layer in a local area become strong enough to support a piled-up array of dislocations of sufficient magnitude that the local stress exceeds the fracture strength of the metal. Because there is a gradient of stress in the surface layer, the crack will propagate until the stress associated with the piled-up array of dislocations is less than the fracture strength. However, during the next cycle(s), the surface-layer stress in front of the crack will again increase, and the process will be repeated. The effects of environment on fatigue life can be explained in terms of their influence on the formation of the surface layer. At reduced pressures, (compared to tests conducted at atmospheric pressures) the surface-layer stress increased more slowly with both strain and number of cycles (Ref 4, 5). In contrast, the surface layer increased very rapidly when the tests were conducted in media that cause corrosion fatigue.

It has also been shown that, for specimens deformed plastically in media that promote corrosion fatigue and stress-corrosion cracking, the dislocation density (determined from activation volume measurement) is also increased.

In applying the surface-layer concept to various plastic flow and fracture phenomena, it is important to realize that the excess work-hardening and resulting high dislocation density are confined to the crystallographic slip planes available. Figure II-1 shows that the dislocation density is highest in the region of the slip bands near the surface and decreases until it becomes uniform in the interior. The depth of the surface layer is given by A in Figure 1a and 1b. In polycrystalline metal at relatively low stresses, all grains may not be plastically deformed, and the excess hardening in the surface layer is confined to those grains that are plastically strained. Furthermore, the amount of excess hardening will vary from region to region because of the orientation of the grains. Similarly, a surface layer may be present at the interface of inclusions, in regions where segregation causes a decrease in strength, and at the bottom of notches or cracks where the stress concentration is high enough to cause plastic deformation.

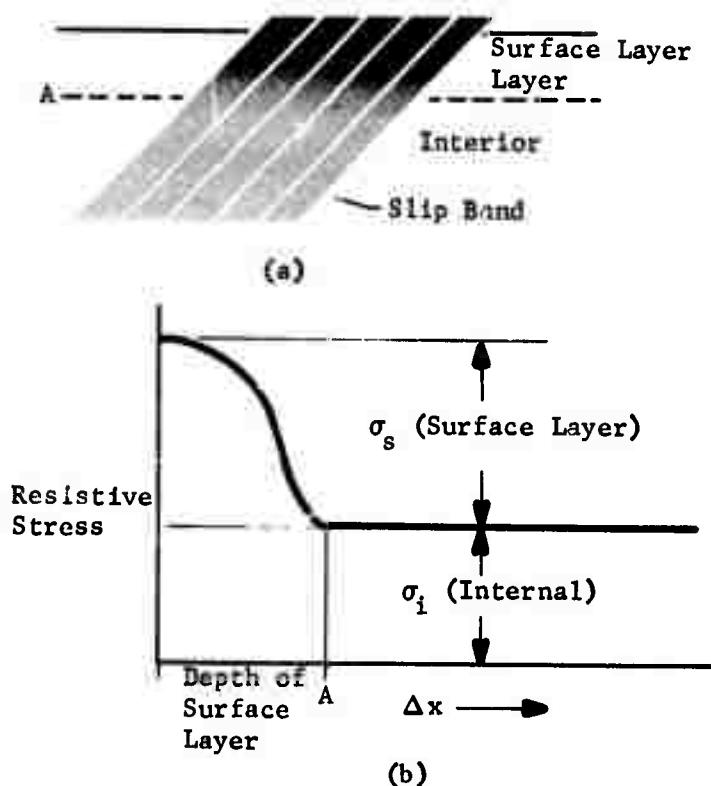


Figure II-1 Schematic Representation of Surface Layer. The gradient in dislocation density is shown in (a) and the average surface layer stress or excess strain hardening is shown in (b)

The excess work-hardening in the surface layer can be measured by determining the difference in the flow stress of a specimen with and without the surface layer (Ref 6). This can be done by straining to a given value and removing the surface by chem-milling. Usually, the removal of about 0.004 in. is enough to eliminate the surface layer. Upon reloading, the plastic flow (measured either by the appearance of slip bands or by the deviation from linearity of the stress-strain curve) starts at a stress lower than that from which the specimen was unloaded. The difference between these two stresses gives the excess work-hardening in the surface layer. This surface-layer stress can be

expressed in terms of the cross-section of the surface layer, σ'_s , or in terms of the entire cross-section of the specimen. In this discussion, the surface-layer stress, σ_s , will be expressed in terms of the entire cross-section. For specimens deformed unidirectionally, our previous measurements indicate that $\sigma'_s \cong 10 \sigma_s$.

The purpose of our research was to show that fatigue failures can be explained in terms of surface-layer stress. This concept is considered valid if fracture (or crack initiation) occurs when the surface-layer stress attains a critical value and no fatigue damage occurs in the interior of the metal during prolonged cycling. A series of experiments were conducted on aluminum 2014-T6 and a titanium alloy (6Al/4V) to measure the work-hardening of the surface-layer stress as a function of the number of stress cycles. In addition, in a set of experiments similar to that conducted by Raymond and Coffin (Ref 7), specimens were fatigued, the surface layer periodically removed by chem-milling, and the fatiguing continued until failure or until the specimen diameter became too small to allow continued testing.

EXPERIMENTAL

The 2014-T6 and 6Al/4V specimens were machined from 5/8-in. diameter rods to a nominal diameter of 0.16 in. and a gage length of 0.30 in. The specimen dimensions and alignment features were in accord with those recommended by Feltner (Ref 8). After machining, the 2014-T6 was stress relieved at 250° for 1 hr. The 6Al/4V was purchased in the annealed condition and was stress relieved at 1300°F in vacuum after machining. Before testing, the specimens were electrochemically polished to remove about 0.004 in. The fatigue tests were conducted in an electrohydraulic machine (MTS) in tension-compression. The upper portion of the specimen was held in alignmatic grips while the lower end was embedded in a fixture containing a low-temperature alloy.

The surface-layer stress was measured by determining the change in the proportional limit. It was found (Ref 5) and verified in our investigation that the proportional limit (as measured by the first deviation of the stress-strain curve from linearity) increased when a specimen was cycled at a constant stress. However, when the surface layer was removed by chem-milling, the proportional limit returned to that of the uncycled specimen. Thus, the increase in proportional limit as a function of number of cycles is equal to the increase in surface-layer stress. The same results can be obtained by linearly plotting the proportional limit against the number of fatigue cycles, N . The difference in value at the intercept at $N = 1/2$ and after cycling gives the surface-layer stress that results from cycling. In these measurements, care was taken to minimize the effect of relaxation of the surface-layer stress. The extensometers were attached immediately after the fatigue cycling, and the tensile tests were started within 1 min after the final cycle.

RESULTS AND DISCUSSION

The load-deformation curve given in Figure II-2 is typical of those obtained after cycling 6Al/4V and 2014-T6 at a constant stress. In the example shown, the stress was 80,000 psi. When cycling was increased from 15,000 to 45,000, the proportional limit increased from 134,000 to 142,000 psi. However, typical of all the cases, the curves coincide at the higher strains. The stress-strain curves for the uncycled and cycled specimens were the same after a plastic strain of about 0.003. A number of experiments were also conducted on both 6Al/4V and 2014-T6 in which the surface layer was removed by chem-milling about 0.01 in. from the diameter after cycling. In all cases, the proportional limit returned to that of the uncycled specimens. These observations reconfirm our

previous conclusions (Ref 5) that, when cycling under constant stress, only the surface layer hardens. In fact, after cycling and removal of the surface layer, the resulting stress-strain curve was indistinguishable from that of uncycled specimens.

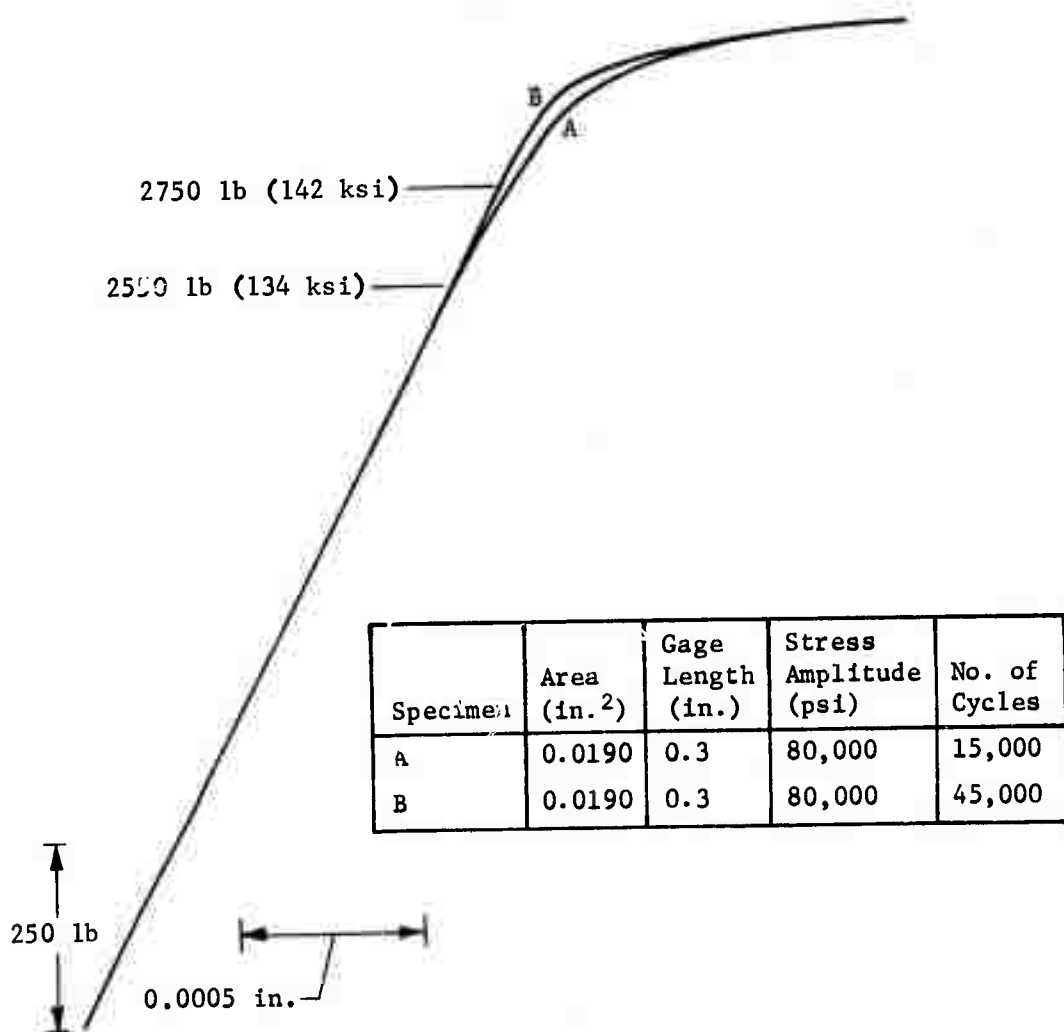


Figure II-2 Typical Load-Deformation Curve

The data in Figures II-3 and II-4 give the relationship between the surface-layer stress, σ_s , and the number of cycles at various stress amplitudes. In all cases, the curves are linear. In the graphs, the asterisks designate the number of cycles required to cause a failure, N_F . Fracture occurred when the surface-layer stress attained a critical value. Within an error of 5%, this critical value is 16,500 psi for the 2014-T6 and 21,500 psi for the annealed 6Al/4V.

Because fatigue failure occurred when the surface layer reached a critical value, it is apparent that the fatigue damage is primarily confined within the surface layer. That is, the damage occurs within those portions of slip bands, etc, that are within a few thousandths of an inch of the surface. If this is the case, it should be possible to postpone fatigue cracking indefinitely by eliminating the surface layer before the critical stress is reached. Specimens of the aluminum and titanium alloys were fatigued for various amounts, ΔN , and then the surface layer was removed by chem-milling 0.010 to 0.003 in. from the diameter (Table II-1), in a manner similar to the experiments of Raymond and Coffin (Ref 7). This process was repeated until the final diameter, D_f , was reached. The specimens were then cycled to failure. The number of cycles required to fail the specimens after the final removal of the surface layer is N_p . The detailed sequences used are given in Figures II-5 and II-6. In these figures, X represents the number of cycles to failure for the uninterrupted tests; 0 denotes that the specimen was removed after the designated number of cycles and 0.010 in. of surface layer chem-milled from the diameter.

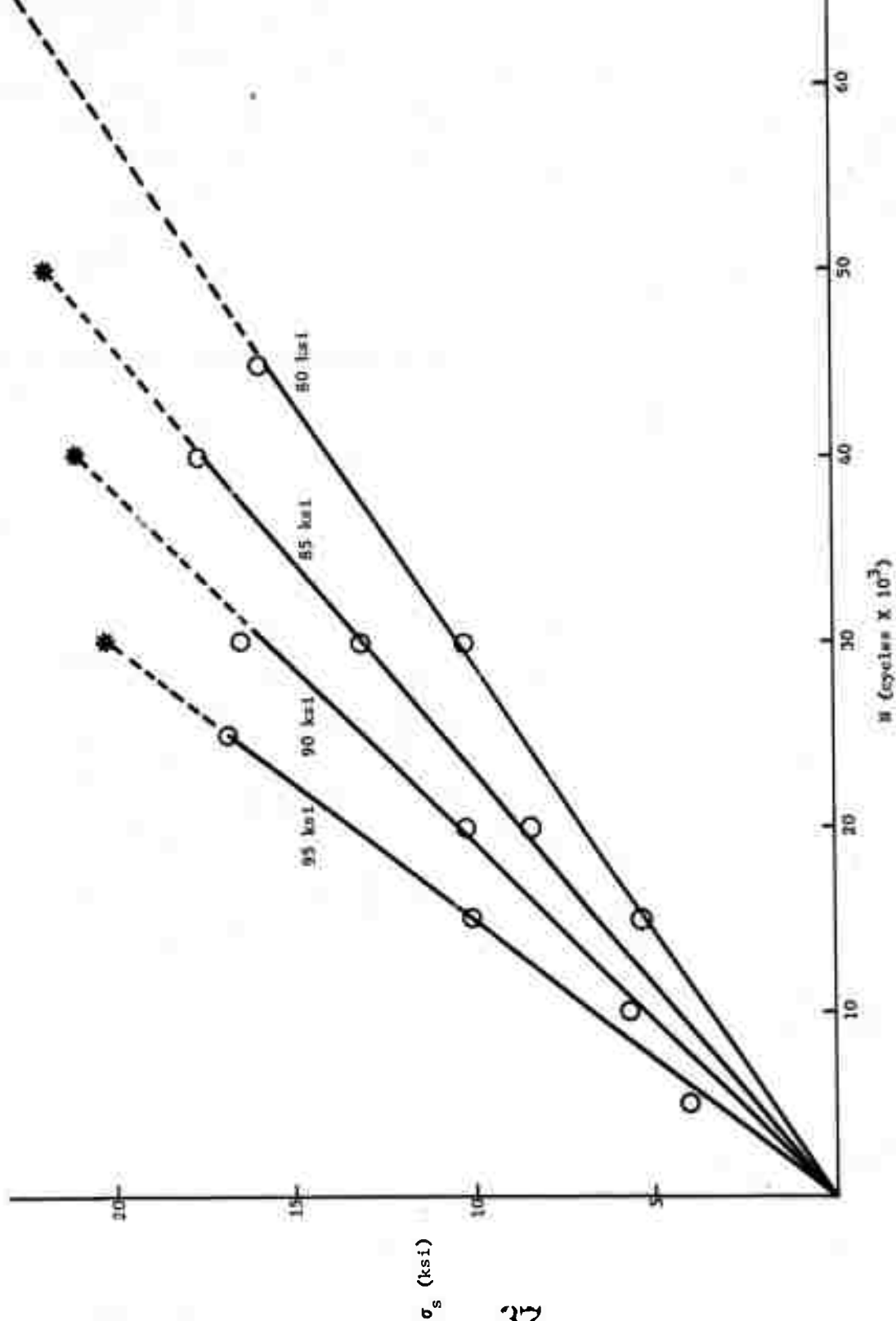


Figure II-3 Increase in Surface-Layer Stress in 6Al/4V Titanium with Number

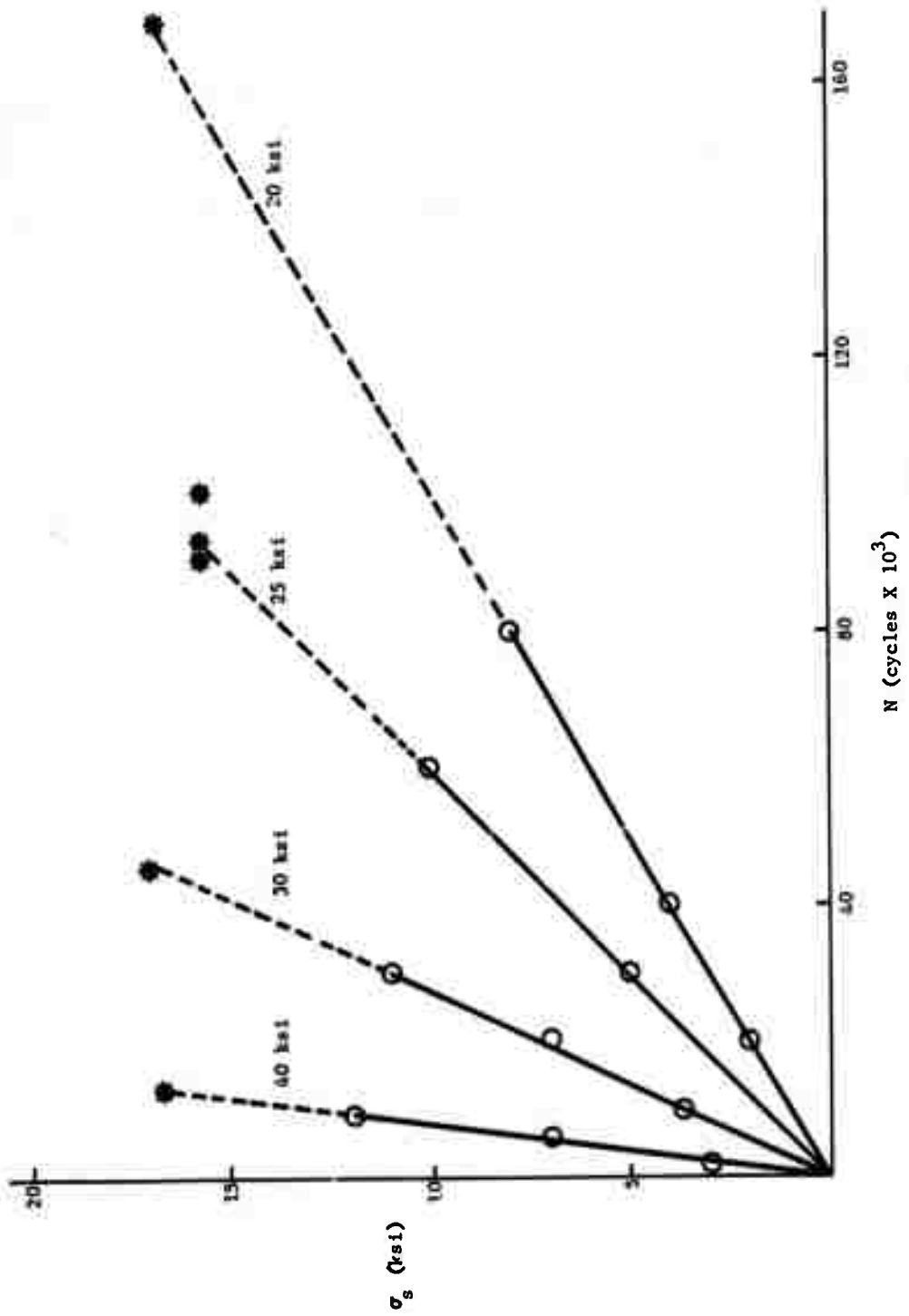


Figure II-4 Increase in Surface-Layer Stress in 2014-T6 Aluminum with Number of Fatigue Cycles and Stress Amplitude, $R = -1$

Table II-1 Extension of Fatigue Life by Removal of Surface Layer

Titanium (6Al/4V)							
Specimen No.	σ (ksi)	N_F	ΔN	$\frac{\Delta N}{N_F}$	N_T	N_P	D_f (in.)
177	80	67,000	20,000	0.3	220,000	100,000	0.0523
178	80	67,000	30,000	0.45	360,000	180,000	0.0411
181	80	67,000	30,000	0.45	150,000	80,000	0.1375
179	90	40,000	12,000	0.30	132,000	63,000	0.0635

2014-T6 Aluminum							
Specimen No.	σ (ksi)	N_F	ΔN	$\frac{\Delta N}{N_F}$	N_T	N_P	D_f (in.)
38	25	95,000	50,000	0.53	500,000	150,000	0.0598
41	40	12,000	6,000	0.5	60,000	56,000	0.0489
36	25	95,000	70,000*	0.74	165,000	--	0.1325
39	25	95,000	60,000*	0.63	100,000	--	0.1460
40	25	95,000	60,000*	0.63	136,000	--	0.1314
*Contained crack after cycling ΔN .							

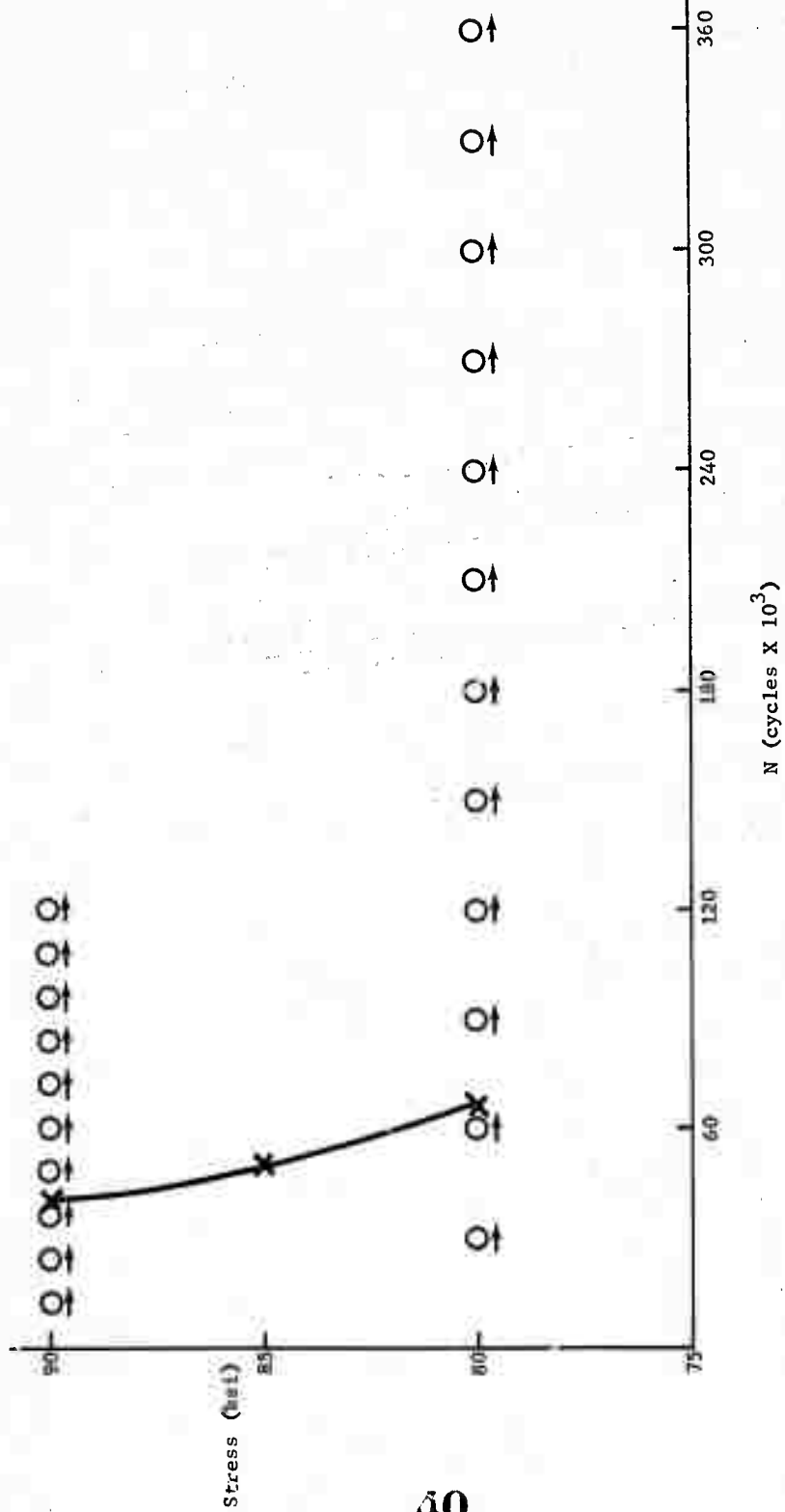


Figure II-5 Increase in 6Al/4V Titanium Fatigue Life by Removal of Surface Layer, $R = -1$

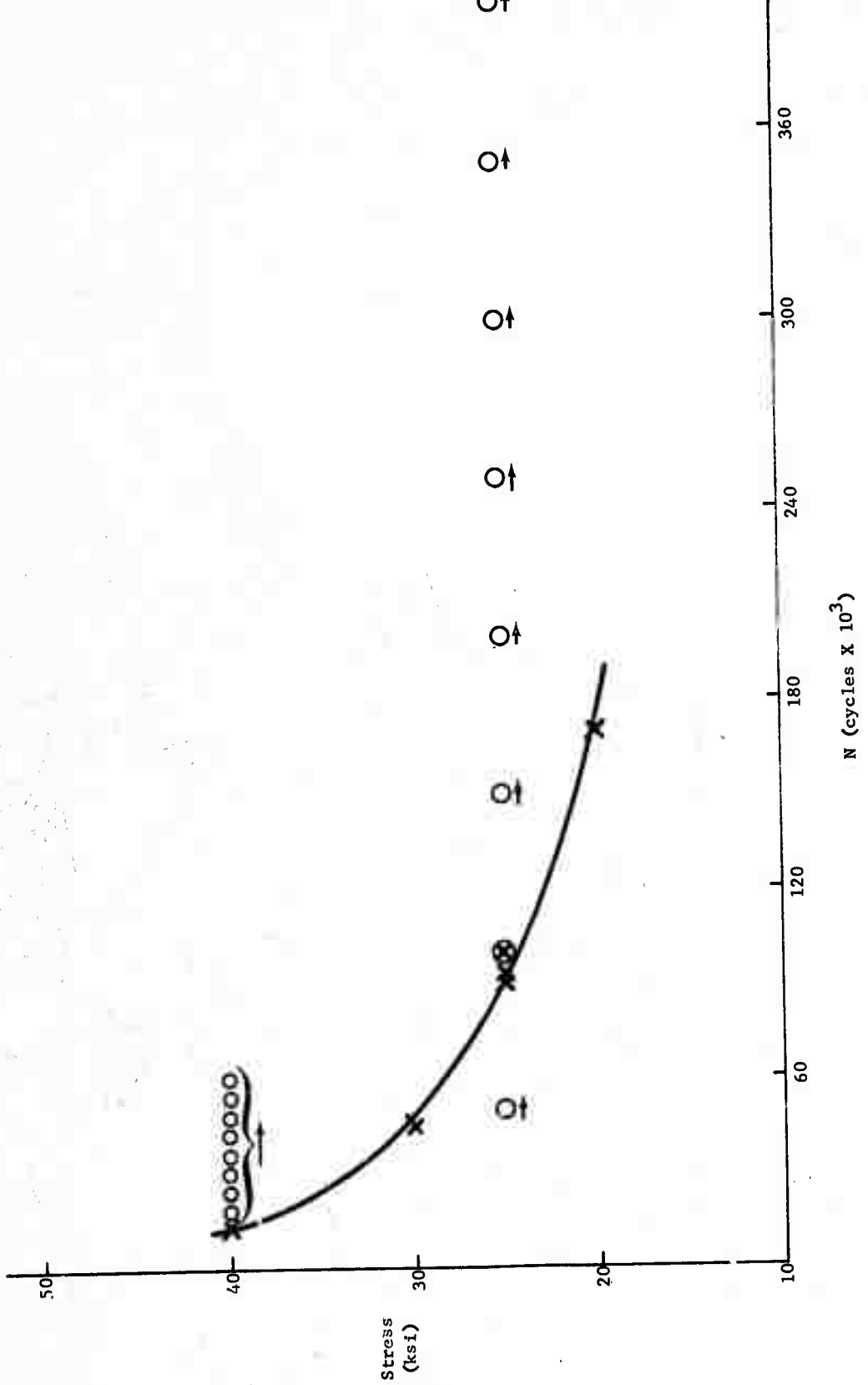


Figure II-6 Increase in 2014-T6 Aluminum Fatigue Life by Removal of Surface Layer, $R = -1$

These data show that, when the specimen was cycled less than about 50% of its normal life, $\frac{\Delta N}{N_F}$, and the resulting surface layer removed, fatigue failure never occurred. After the specimens had been cycled N_T times and then fatigued to failure after first removing the surface layer, the number of cycles for failure, N_P , was always greater than that required to fail the specimens in the uninterrupted tests, N_F . That is, $N_P > N_F$, even though the specimens were cycled as much as ten times their normal life. This indicates that no fatigue damage occurred in the interior of the specimen.

Specimens 36, and 40, which were cycled ΔN times for about 60 to 70% of the life, N_F , did not show much improvement when the surface layer was removed. Examination of these specimens after the first fatigue period showed that cracking had occurred. Examination of the fractured surfaces as well as the outer surfaces of the other specimens after each ΔN period failed to reveal any signs of cracks. It was concluded (except as noted) that the removal treatment eliminated only the surface layer, not the cracks. In some cases, ΔN was only about 30% of the fatigue life, and cracks are not expected to form at such a low number of cycles.

On the basis that fatigue failure will occur when the surface-layer stress reaches a critical level, a relationship between the stress amplitude and cycles to failure can be derived. From Figures II-3 and II-4:

$$\sigma_s^* = C_s^* = S N_F \quad [1]$$

$$\text{where } S = \frac{d\sigma_s}{dN} \quad [2]$$

The change of S with stress amplitude obtained from the data in Figures II-3 and II-4 is given in Figure II-7 and shows that:

$$S = k \sigma^P .$$

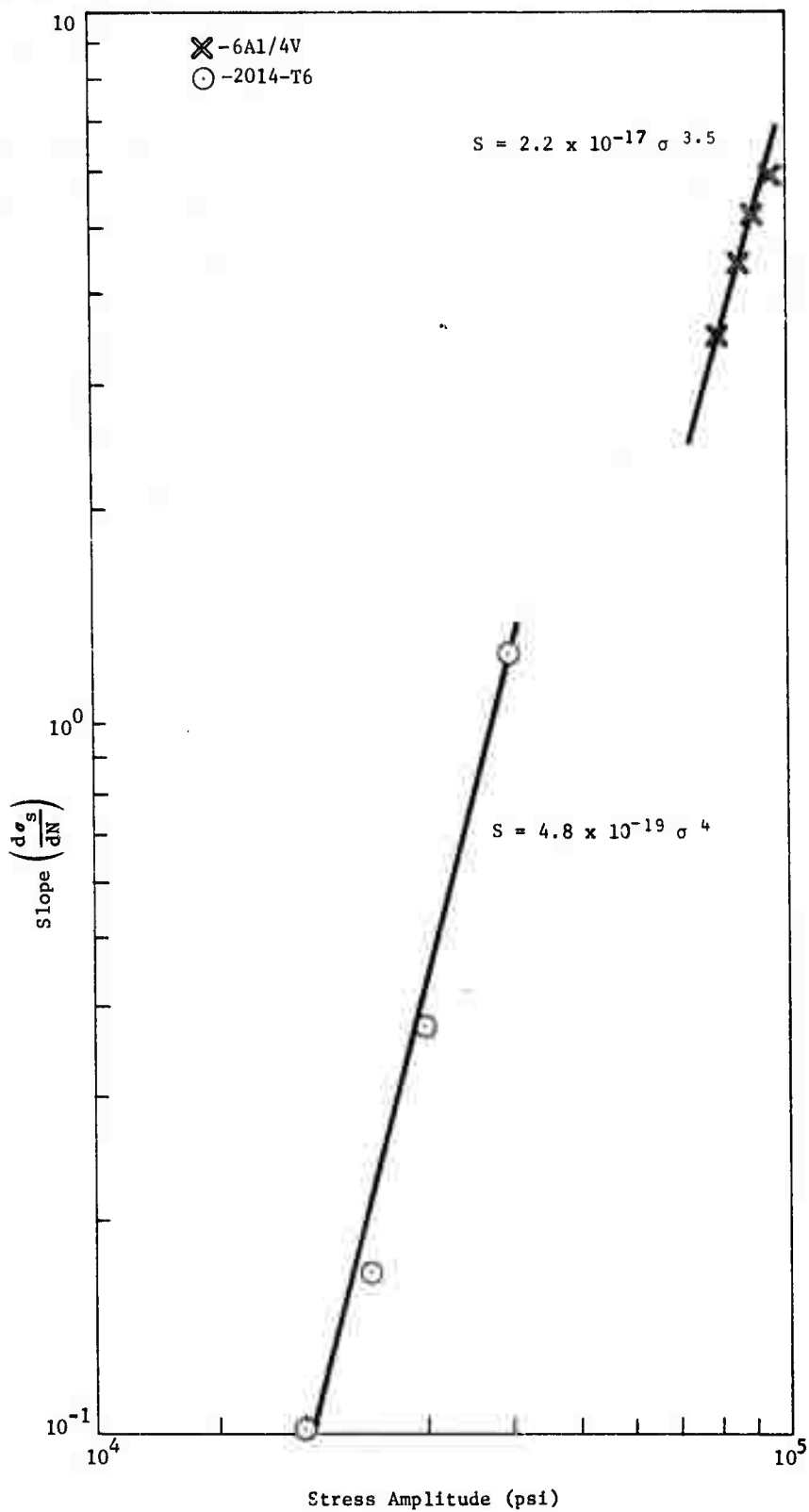


Figure II-7 Relationship between Slope $S = d\sigma_s/dN$ and Stress Amplitude

From Equations 1 and 2

$$\frac{\sigma}{S} = \frac{C \sigma}{S} = k \sigma^p N_F^p \quad [3]$$

or

$$\sigma = \left(\frac{C \sigma^*}{N_F k} \right)^{\frac{1}{p}} \quad \text{and} \quad b = \frac{1}{p} \quad [3a]$$

Equation 3 implies a linear curve when the fatigue data are plotted in terms of $\log \sigma$ and $\log N$. This is in agreement with the results reported by Basquin (Ref 9). The fatigue data for the specimens used in this investigation also conform to this relationship (Figure II-8). In particular, for 6Al/4V:

$$S = 2.2 \times 10^{-17} \sigma^{3.5} \quad [4]$$

$$\text{and } \sigma = 10^6 N_F^{-0.3}. \quad [5]$$

From the fatigue curves

$$\sigma = 1.3 \times 10^6 N_F^{-0.25}. \quad [6]$$

For the 2014-T6:

$$S = 4.8 \times 10^{-19} \sigma^4 \quad [7]$$

and

$$\sigma = 4.3 \times 10^5 N_F^{-0.25} \quad [8]$$

From the fatigue curve

$$\sigma = 5.2 \times 10^5 N_F^{-0.27}. \quad [9]$$

The agreement between the equations derived from the surface-layer concept and the experimental fatigue data is considered good; compare Equation 5 with 6 and 8 with 9.

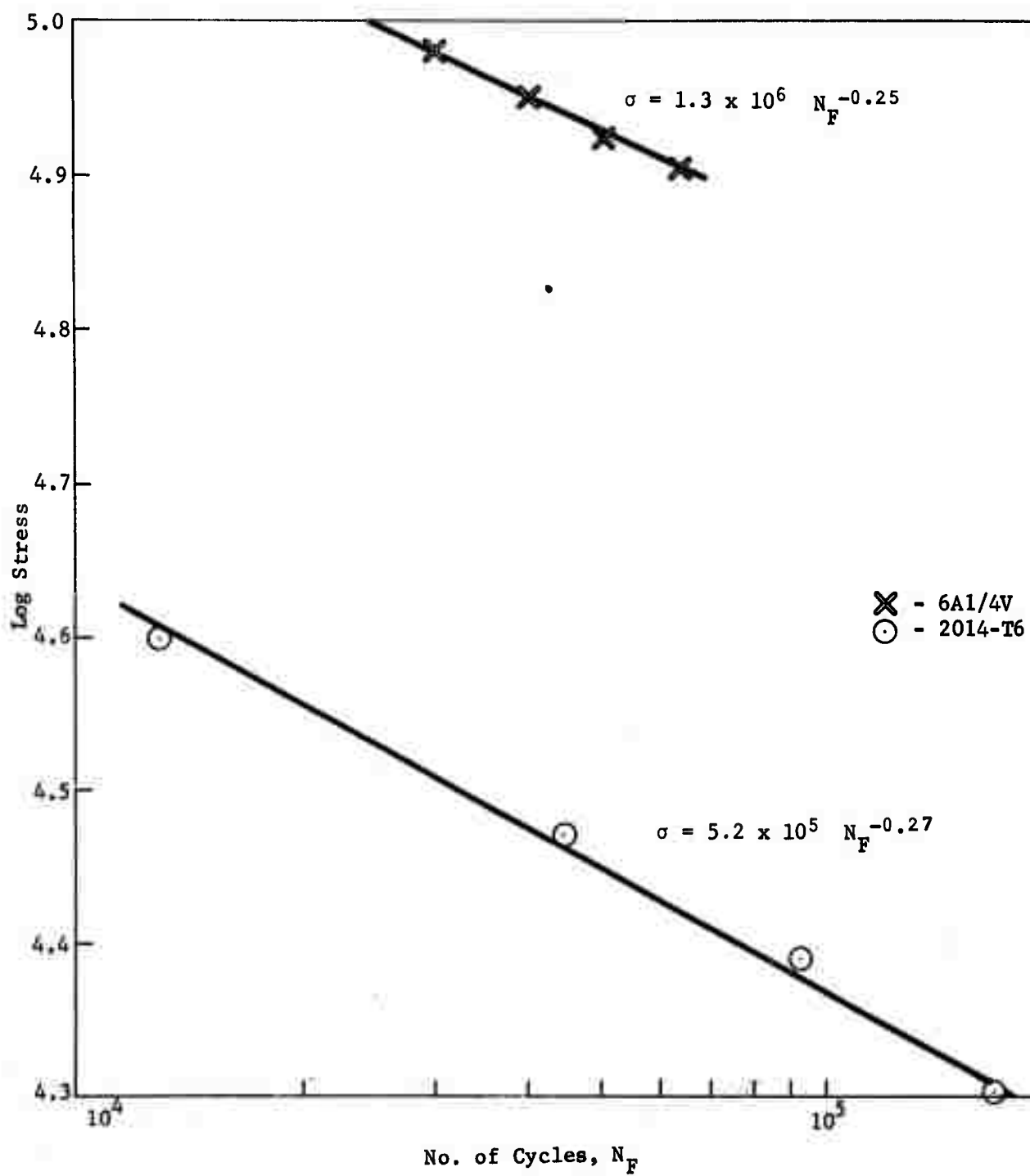


Figure II-8 Relationship between Fatigue Life and Stress Amplitude

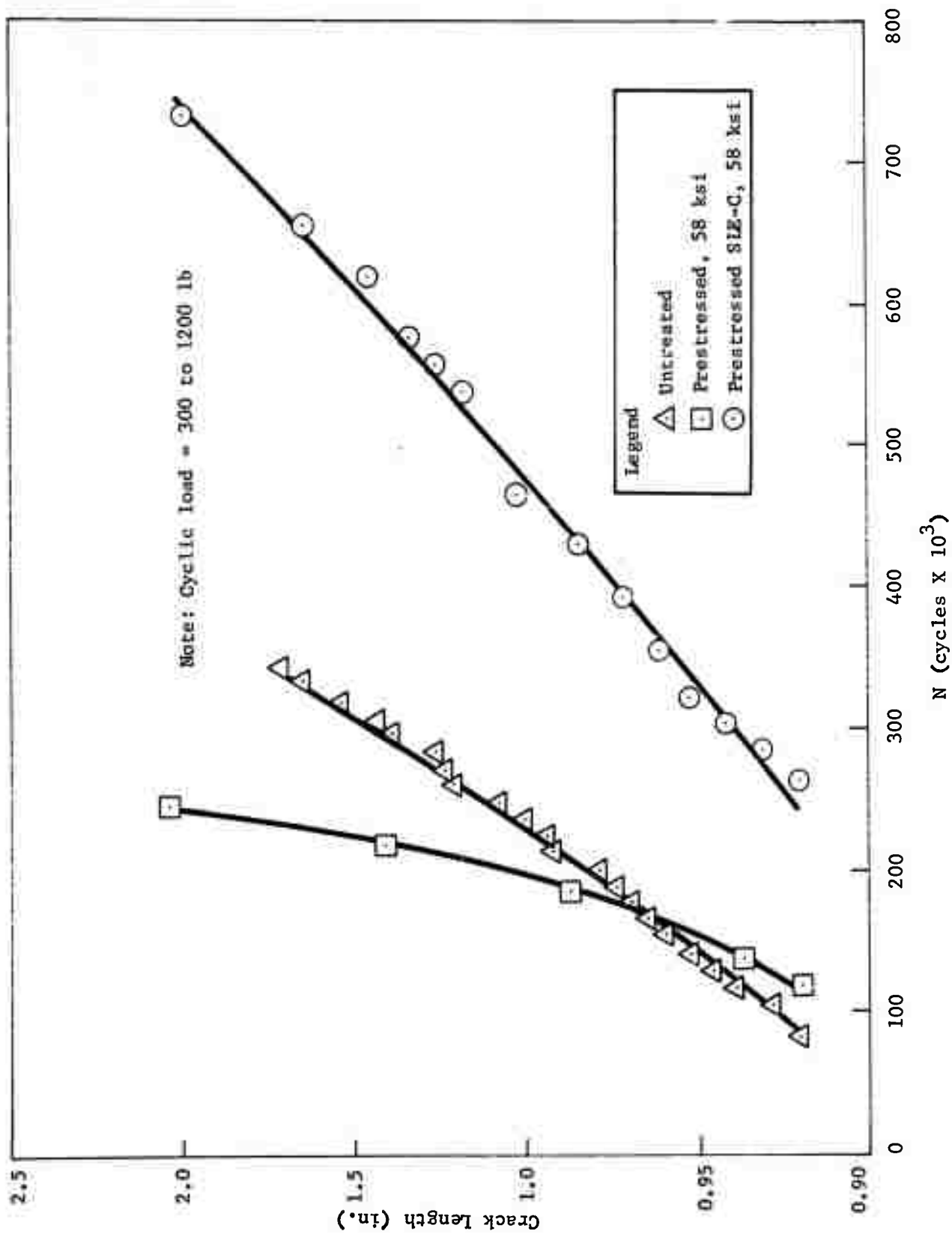


Figure II-9 Crack Propagation Behavior of 2014-T6 under Plane Strain Conditions,

In considering Equation 3 to describe fatigue, both initiation and propagation should be taken into account. For the specimen size and materials used, the ratio $N_o/N_F \cong 0.6$. However, it is suspected that, when $N_F \gg N_o$, Equation 3 may have to be modified to include the number of cycles required to propagate the crack to produce failure. In this case, Equation 3 would still apply to the initiating phase, with $N_F = N_o$, and the constant $C^* = \sigma^*$ would be lowered.

The concept that fatigue failures are primarily associated with local stress fields in the surface layer appears to be in agreement with other observations. This is especially true when it is considered that accumulation of dislocations within the surface layer is primarily within the slip bands. Thus, cracks that start at slip bands or at intrusions and extrusions are manifestations of the surface layer. The prolonged life obtained by chem-milling and the fact that, after prolonged cycling, the interior of the specimen has a fatigue life greater than that in the uninterrupted tests, show that fatigue damage is not confined to the surface itself. Rather, experiments demonstrate that approximately 0.003 in. must be removed before the damaged region is eliminated. In contrast, removing large amounts of metal (up to 0.015 in.) does not improve the fatigue life more than removing 0.003 in. Thus, it would appear that fatigue damage is confined to a region approximately 0.003 in. from the surface. This distance can be expected to vary with specimen size and, perhaps, stress amplitude. The environment may also affect this depth.

The influence of the surface layer on fatigue can be demonstrated by determining the rate of crack propagation, da/dN , on compact tension specimens of 2014-T6 treated to obtain various degrees of surface-layer conditions. Bars of the alloy were pre-stressed to 58,000 psi and machined into specimens. In some cases, the surface layer was removed by chem-milling. In this treatment,

termed SLE (Surface Layer Eliminated), the surface layer formed during fatigue cycling is much smaller than in the untreated specimen. The specimens prestressed to 58,000 without chem-milling have a surface-layer stress higher than that of the untreated specimens. Although only a small part of the advancing crack passes through the outer surfaces of the specimen, Figure II-9 and II-10 show that the surface layer has a pronounced effect on the rate of crack propagation. For the SLE specimen, the number of cycles required to start crack propagation was increased from about 100,000 to 250,000. Crack propagation rate was also reduced. For specimens with large surface-layer stresses, the crack propagation rate is much greater, although initiation of crack propagation requires about the same number of cycles as for untreated specimens.

Similar effects were obtained from 6Al-4V under plane stress conditions. As shown in Figure II-11, decreasing the surface-layer stress decreased the rate of crack propagation (Curve B) compared to the untreated specimens (Curve A), while increasing the surface-layer stress increased the crack propagation rate (Curves C and D).

SUMMARY

During fatigue, the surface layer work-hardens and, when surface-layer stress reaches a critical value, fracture occurs. By periodically removing the work-hardened surface layer after fatiguing, the fatigue life was prolonged and the interior did not suffer fatigue damage as a result of the prolonged cycling. The resulting experiments show that fatigue can be expressed as

$\sigma = aN_F^b$ where $b = -0.25$ and -0.27 for titanium (6Al/4V) and aluminum 2014-T6, respectively.

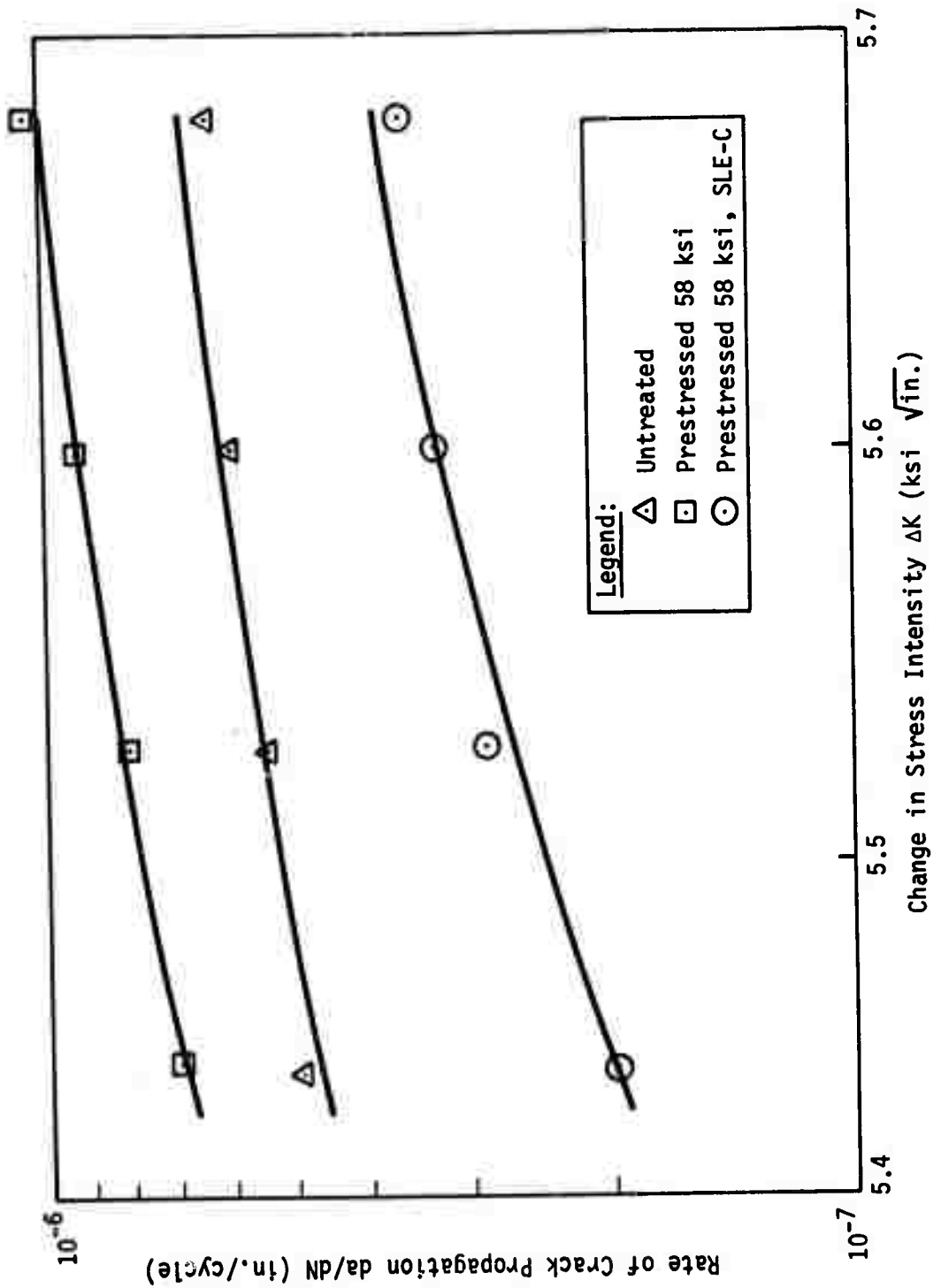


Figure II-10 Crack Propagation Behavior of 2014-T6 under Plane Strain Conditions, Compact Tension Specimens 1-in Thick

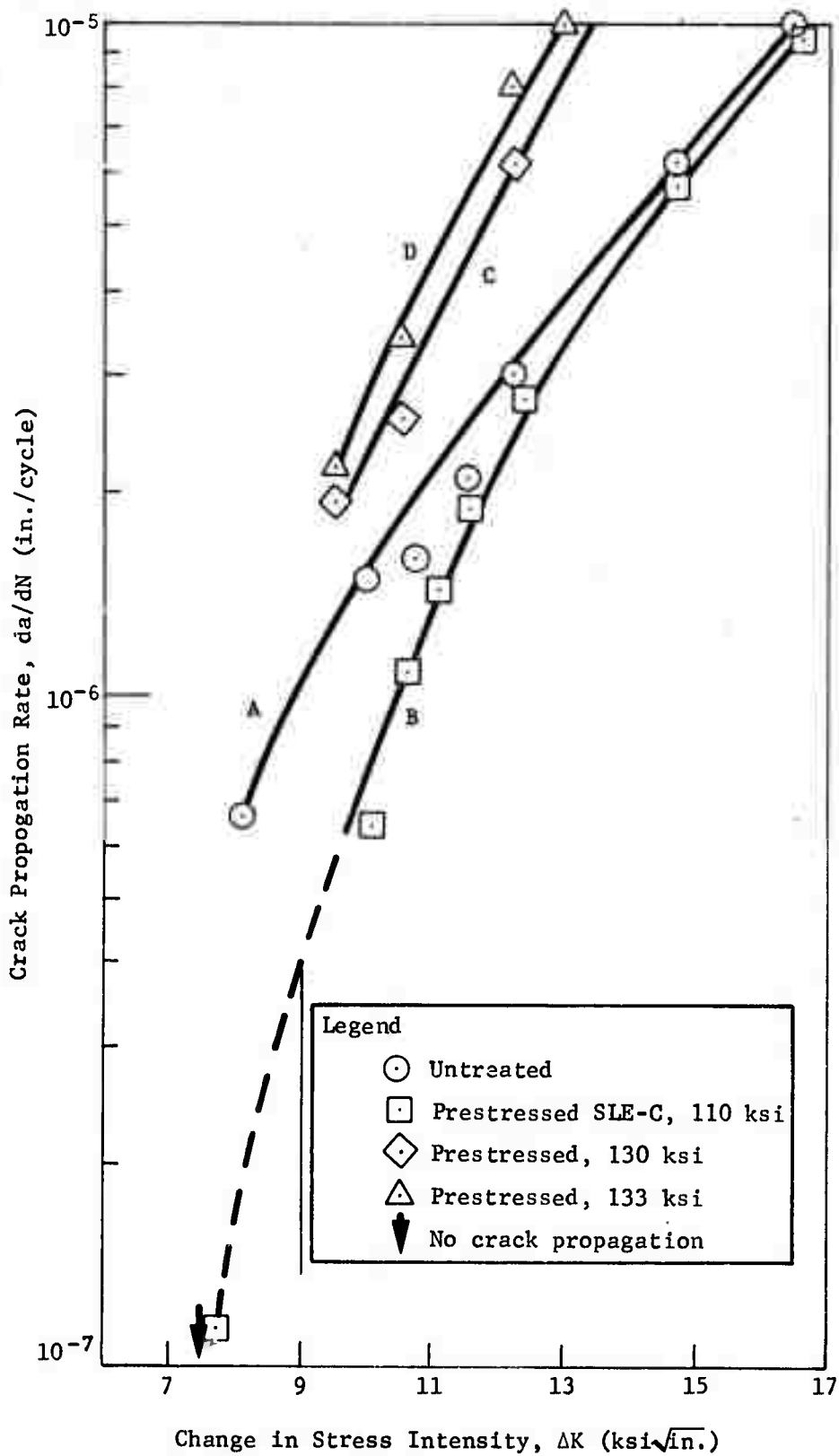


Figure II-11 Crack Propagation Behavior of 6Al-4V under Plane Stress Conditions, Center-Cracked Specimens 0.067-in. Thick

Excellent agreement for fatigue life was obtained between the results derived from the σ_s values and experimental fatigue data.

It is assumed that fatigue cracks occur when, on appropriate slip or cleavage planes within the surface layer, the local stress from piled-up arrays of dislocations exceeds the fracture stress. Environmental effects can be explained in terms of their influence on surface-layer stress. Environments that increase surface-layer stress decrease fatigue resistance; environments that decrease surface-layer stress increase fatigue resistance.

REFERENCES

1. I.R. Kramer, "Fundamental Phenomena in the Material Sciences", Volume 3 (Surface Phenomena) p. 171, Plenum Press, 1966.
2. H. Shen, S. Podlaseck and I.R. Kramer, Acta Met, 14, (1966), 341.
3. H. Shen and I.R. Kramer, Trans. Inter. Vac. Met. Conference, 1967, p. 263
4. I.R. Kramer, Trans. ASM, 62 (1969), 521.
5. I.R. Kramer, Proc. Air Force Conf. on Fatigue and Fracture, Dec., 1969, AFFDL-TR-70-144, p. 271.
6. I.R. Kramer, Trans. Met Soc., 233 (1965) 1462.
7. M.H. Raymond and L.F. Coffin, Jr., Acta. Met. 11 (1963), 801.
8. C.E. Feltner and M.R. Mitchell, ASTM STP 465, p. 27.
9. O.H. Basquin, Proc. ASTM, 10 (1910), 625.

III. Surface-Layer Stress at Notches

INTRODUCTION

Surface-layer stress has been measured on a number of metals. However, in all cases, the measurements were made on smooth specimens. The values were obtained either by denoting the change in initial flow stress after prestraining and chemical removal of the surface layer or by eliminating it by a relaxation treatment. Based on smooth-specimen data, the surface-layer stress has proved useful in explaining crack initiation and propagation in various environments such as vacuum and those that cause corrosion fatigue and stress corrosion. However, in many applications, a stress concentration is present and it is important to determine the extent to which notches, etc. influence the surface-layer stress. To be consistent with the concept that the surface layer decreases the ductility, it would be expected that the stress concentrations would enhance the formation of the surface layer at the bottom of the notches.

Another important parameter of the surface layer is its ability to relax. In some case (for example, aluminum, copper, gold, and 6Al/4V titanium) the surface layer will disappear completely by a relaxation mechanism at low temperature. However, in alloys like 7075-T6 and 2014-T6 aluminum, the dislocations in the surface layer are so strongly pinned that relaxation of the surface layer will not occur until the temperature is raised to a point where overaging in the bulk also takes place. The relaxation aspect of the surface layer is important for two reasons. First, it provides a practical method for eliminating the layer. Second, in this investigation, to measure the surface-layer stress, chem-milling or machining cannot be used because of the errors they may introduce. The relaxation method can be used without introducing changes in the notch geometry. For this reason, our investigation was confined to titanium (6Al/4V).

EXPERIMENTAL PROCEDURE

The material used in this investigation was titanium (6Al/4V) extruded rod, 3/4-in. diameter. The rods were purchased annealed and were machined into tensile specimens (Figure III-1). Notches with flank angles of 90, 60 and 30° were machined with a preformed cutter, and the specimens were stress-relieved at 1300°F in a vacuum furnace ($\sim 10^{-6}$ torr). The tensile tests were conducted in a 50,000-lb capacity Baldwin machine. The strains were measured by a diametral gage equipped with knife edges that fitted inside the notch. The diametral gage was taken from the design recommended by Hirschberg (Ref 1). A linear variable differential transformer was used to record the deformation. Load and deformation were recorded on an X-Y plotter with a scale of 1 in. = a load of 1500 lb and a diametral strain (ϵ_d) of 0.009.

The surface-layer stress was measured by taking the difference between the unloading stress and the initial stress upon reloading after eliminating the surface layer. To determine the time required to eliminate the surface layer, five specimens with a 60° notch were strained to $\epsilon_d = 0.01$ and allowed to relax for periods of 1 to 24 hr. After the 1 hr, no further change in surface-layer stress was detected. Relaxation of the surface-layer stress at room temperature was then systematically investigated in the interval from 0.5 to 60 min.

RESULTS

The surface-layer stress of notch specimens as a function of diametral strain, ϵ_d , is shown in Figure III-2. For all three cases, the curves followed the equation $\sigma_s = a \epsilon^n$. In particular, in terms of the notch angle.



Note: All dimensions in inches.

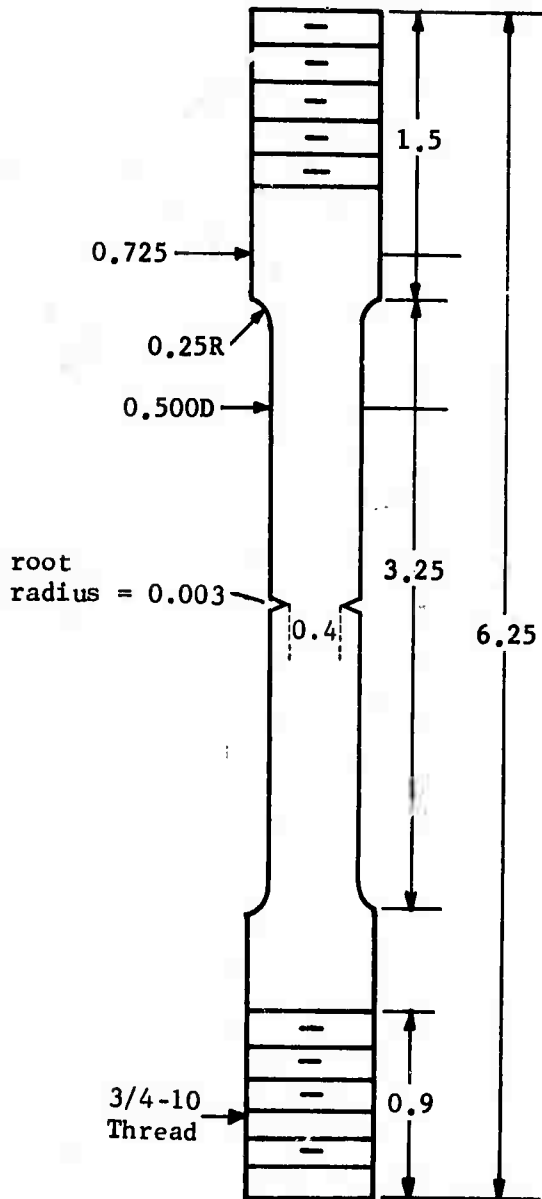


Figure III-1 Configuration of Notched Tensile Specimen

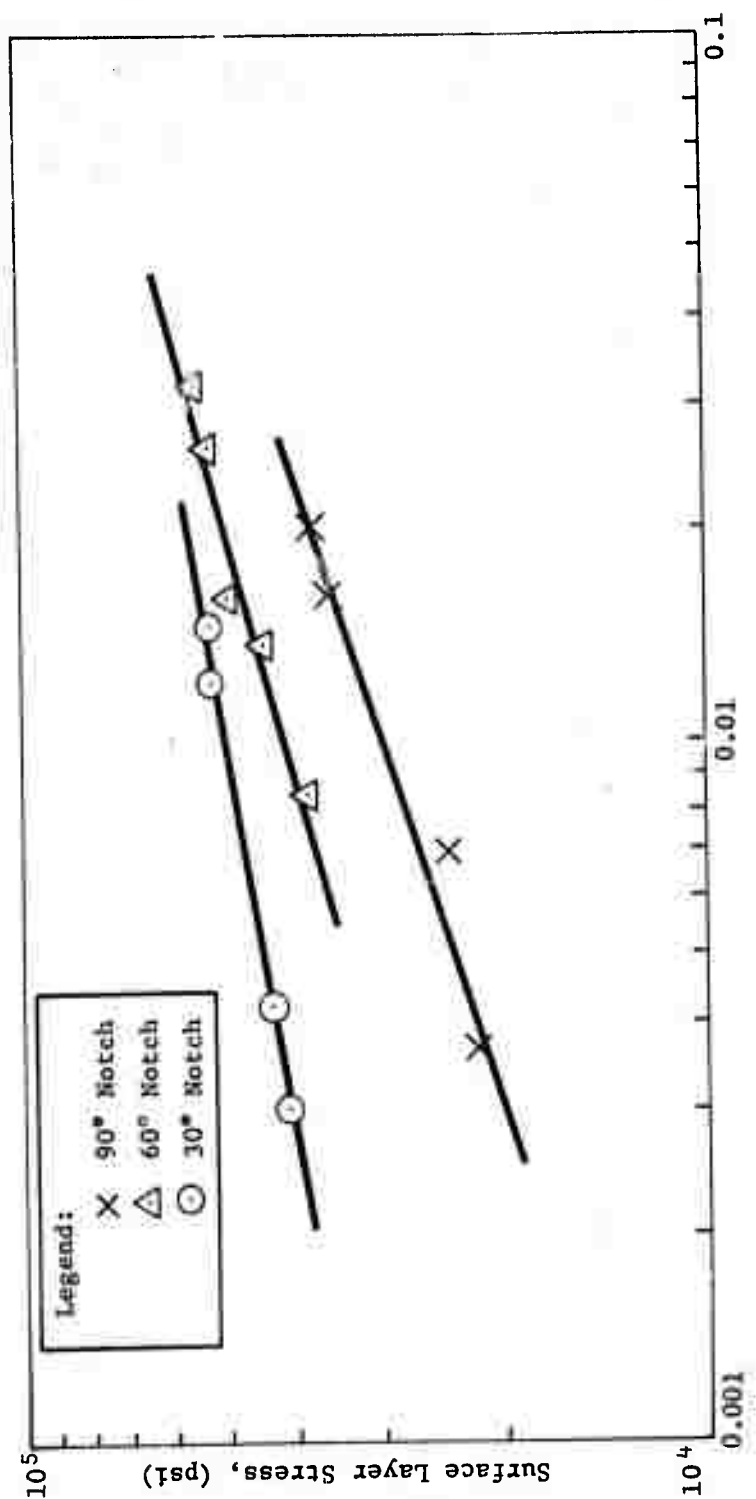


Figure III-2 Effect of Notches on Surface-Layer Stress of 6Al/4V

$$\sigma_s = 1.1 \times 10^5 \epsilon_d^{0.18} \text{ for } 30^\circ \text{ notch}$$

$$\sigma_s = 1.35 \times 10^5 \epsilon_d^{0.26} \text{ for } 60^\circ \text{ notch}$$

$$\sigma_s = 1.4 \times 10^5 \epsilon_d^{0.33} \text{ for } 90^\circ \text{ notch}$$

for the unnotched specimen

$$\sigma_s = 6.3 \times 10^4 \epsilon_d^{0.4}$$

As expected, the data show that surface-layer stress is increased markedly by stress concentrators. Compared to the unnotched specimen, the surface-layer stress at $\epsilon_d = 0.01$ is increased by factors of 3, 4, and, 5 for notches of 90, 60 and 30° respectively. Note that the constant, a , for the notched specimens is essentially the same. However, the exponent, n , changes from 0.18 to 0.33 as the flank angle increases from 30 to 90°.

The rate of relaxation of specimens with 60° notches is shown in Figure III-3. As in previous results, a linear relationship was found when $\log \frac{\Delta \sigma_s}{\sigma_s(0)}$ was plotted with respect to $\log t$. Note that the rate of relaxation is the same for notched and unnotched specimens.

The observation that the surface-layer stress increases markedly at the root of notches is consistent with other observations of parameters that decrease ductility. Previous investigations (Ref 2) have shown that environments that promote stress corrosion cracking and corrosion fatigue damage increase the surface-layer stress, while "friendly" environments (e.g., vacuum) decrease surface-layer stress. These results support the general concept that crack propagation and formation are strongly influenced by the surface layer. It is proposed that the surface layer consists of a large number of dislocations at the ends of the slip bands. This layer acts as a barrier to the motion of other dislocations. Thus,

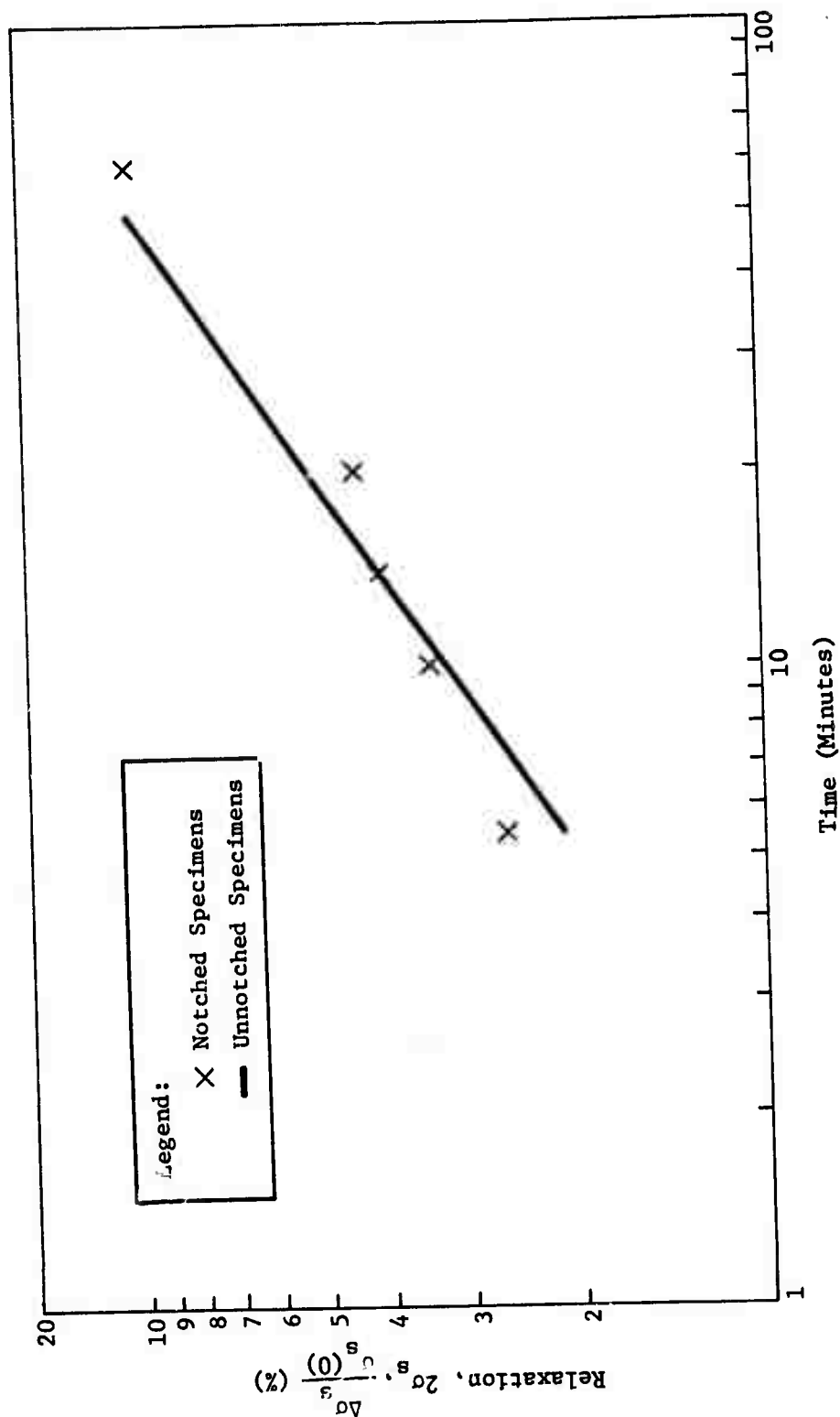


Figure III-3 Relaxation of Surface-Layer Stress of 60° Notched Specimens of 6Al/4V, $R = -1$

during plastic deformation, dislocations can pile up against this barrier. As a result of strain or fatigue cycling, the surface-layer strength increases. Fracture will occur when the stress field associated with the piled up array exceeds the fracture strength of the material.

REFERENCES

1. M.H. Hirschberg. Manual on Low Cycle Fatigue Testing ASTM. STP 465 (1969).
2. I.R. Kramer. Trans. ASM 62 (1969) 54.

IV. Crack Propagation in an Iron-Silicon Alloy

INTRODUCTION

Prestressing a metal to its proportional limit and eliminating the surface layer formed during prestressing improves the mechanical behavior of materials. The results of this treatment, known as the S-SLE (Stressed and Surface Layer Eliminated), on fatigue (Ref 1) and creep (Ref 2) properties have been studied. This technique is successful because, when a metal is deformed, the surface work-hardens to a greater extent, and the surface layer has a higher density of dislocations than the interior. The high dislocation content of the surface layer is undesirable, and its removal results in material with better mechanical properties. Although indirect evidence for these ideas is available (Ref 3), it was considered desirable to get quantitative information on a model material. The Iron-silicon alloy (Fe-3% Si) was chosen because etch-pitting techniques had been developed to reveal dislocation densities, distributions (Ref 4) and plastic zones (Ref 5).

The dislocation density distribution as a function of depth from the surface has been obtained and discussed in Chapter I. These results confirm that the surface layer is indeed a region of higher dislocation density. The removal of such a layer should result in substantial improvements in mechanical properties like crack resistance. It was therefore decided to study fatigue crack propagation in specimens of Fe-3% Si with and without the surface layer. The plastic zone was characterized by etch-pitting studies and study of the dislocation gradient in the vicinity of crack. No such measurements have been reported in the literature. Klesnil and Lukas *et al* (Ref 6) studied crack fronts by transmission electron microscopy and reported that the plastic zone around the propagating fatigue crack in copper consists of a very fine highly oriented cell structure. The minimum cell size is on the order of tenths of microns.

EXPERIMENTAL TECHNIQUES

The Fe-3% Si was obtained from U. S. Steel through the courtesy of W.C. Leslie. The composition is given below.

Element	<u>C</u>	<u>Mn</u>	<u>P</u>	<u>S</u>	<u>Si</u>	<u>Cu</u>	<u>Ni</u>	<u>Cr</u>	<u>Mo</u>	<u>Sn</u>	<u>Al</u>
wt, %	0.025	0.08	0.005	0.019	3.14	0.01	0.02	0.02	0.002	0.013	0.0

Specimen Preparation and Heat Treatment

The material was received as hot-rolled. A number of heat-treating procedures were tried because the etch-pitting characteristics critically depend on the carbon content. The Battelle Si-Fe discussed in Chapter I required annealing at 1436°F for 4 hr, followed by forced-air cooling to room temperature. However, this treatment for the U. S. Steel material did not result in good etching characteristics. Consequently, five trial runs were made as follows. Specimens were annealed for 15 min at 1200, 1300, 1400 and 1600°F and then water-quenched. At least 0.01 in. was removed from the surface to eliminate any decarbonized layer and the specimens were polished with 1- μ diamond paste. A hardness indentation was made on each specimen to produce deformation. It was then aged to allow migration of carbon atoms in solution to dislocations. Then the localized enrichment of carbon atoms would cause the regions around dislocations to etch preferentially. A treatment of 20 min at 300°F accomplished this aging without significantly altering dislocation arrangements produced by the deformation. Specimens were then etched electrolytically in the Morn's solution (Ref 7) (7 ml H₂O, 25 g chromium trioxide, and 133 ml glacial acetic acid). A stainless-steel cathode was used. The voltage-current curve was obtained (Figure IV-1) and found to have a plateau at 11 V and 3 to 5 A. Consequently, etching was done at 11 V and metallographic observations showed that etching

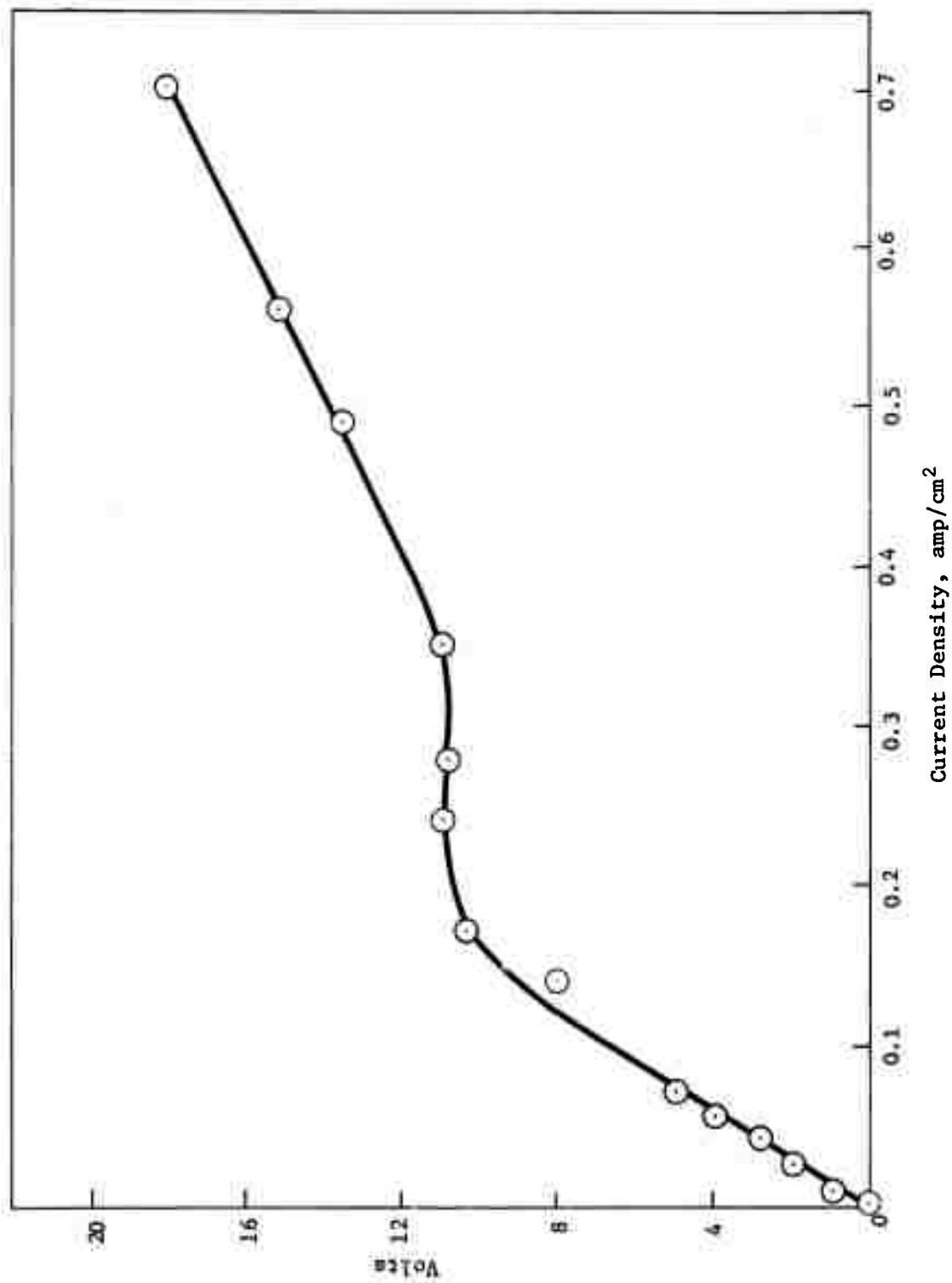


Figure IV-1 Voltage-Current Density Curve for Electrolytic Etching of Fe-3% Si

characteristics were the best for the material water-quenched from 1400°F. Hence, it was decided to use this treatment on specimens for fatigue crack propagation studies. Specimens were wrapped in Sen-Pak foils, annealed at 1400°F for 15 min and water-quenched. Any decarbonized layer present was removed by eliminating 0.01 in. from the surface.

Specimen Configuration

Center-cracked plane-stress specimens were used for this study. Specimen configuration is shown in Figure IV-2.

Testing

All cyclic loading tests were conducted in MTS electrohydraulic machines. A sinusoidal pulse was used, and the load was monitored by a load cell. The prestressing to 50 ksi (the proportional limit) was done in a Baldwin (50,000-lb) machine on Fe-3% Si plates, and specimens were machined from these. The surface layer was chemically removed to a depth of 0.006 in. from each surface. A 0.125-in.-diameter hole was then drilled, and the wings of the initial flaw were formed by a jeweler's saw.

Crack length was measured with a traveling microscope to an accuracy of ± 0.0001 in. The number of cycles to initiate the crack was measured for the untreated and treated specimens. The crack length, 2σ , was measured as a function of number of cycles, N . Specimens were cycled at 20 Hz between loads 783 to 3,133 lb or stresses 6,250 to 25,000 psi

Metallography

After 500,000 cycles, and the curve for crack length versus number of cycles was obtained, the specimens were metallographically examined. The fatigued specimens were aged to allow segregation of carbon atoms to dislocations and etched to reveal these dislocations as described earlier.

RESULTS AND DISCUSSION

The results of crack propagation studies on untreated and treated specimens of Fe-3% Si are summarized in plots of (a) crack half length, a , versus number of cycles, N , and (b) the rate of crack propagation, da/dN , versus the change in stress intensity factor, ΔK . The stress intensity change, ΔK , for the specimen used was calculated as

$$\Delta K = \frac{\Delta L}{B} \frac{a}{W} F \quad [1]$$

where

ΔL - difference in maximum and minimum load

W - width of specimen

B - thickness

$2a$ - crack length

and

$$F = W \tan \frac{\pi a}{W}$$

The ratio $R = K_{\min}/K_{\max}$ was held constant at 0.25. The results were obtained for a frequency of 20 Hz.

Crack length, $2a$, as a function of number of cycles, N , is plotted in Figure IV-3 for Fe-3% Si center-notched specimens 0.063-in. thick. The specimens were cycled at 20 Hz between 6,250 and

Cyclic Stress 6,250 to 25,000 psi

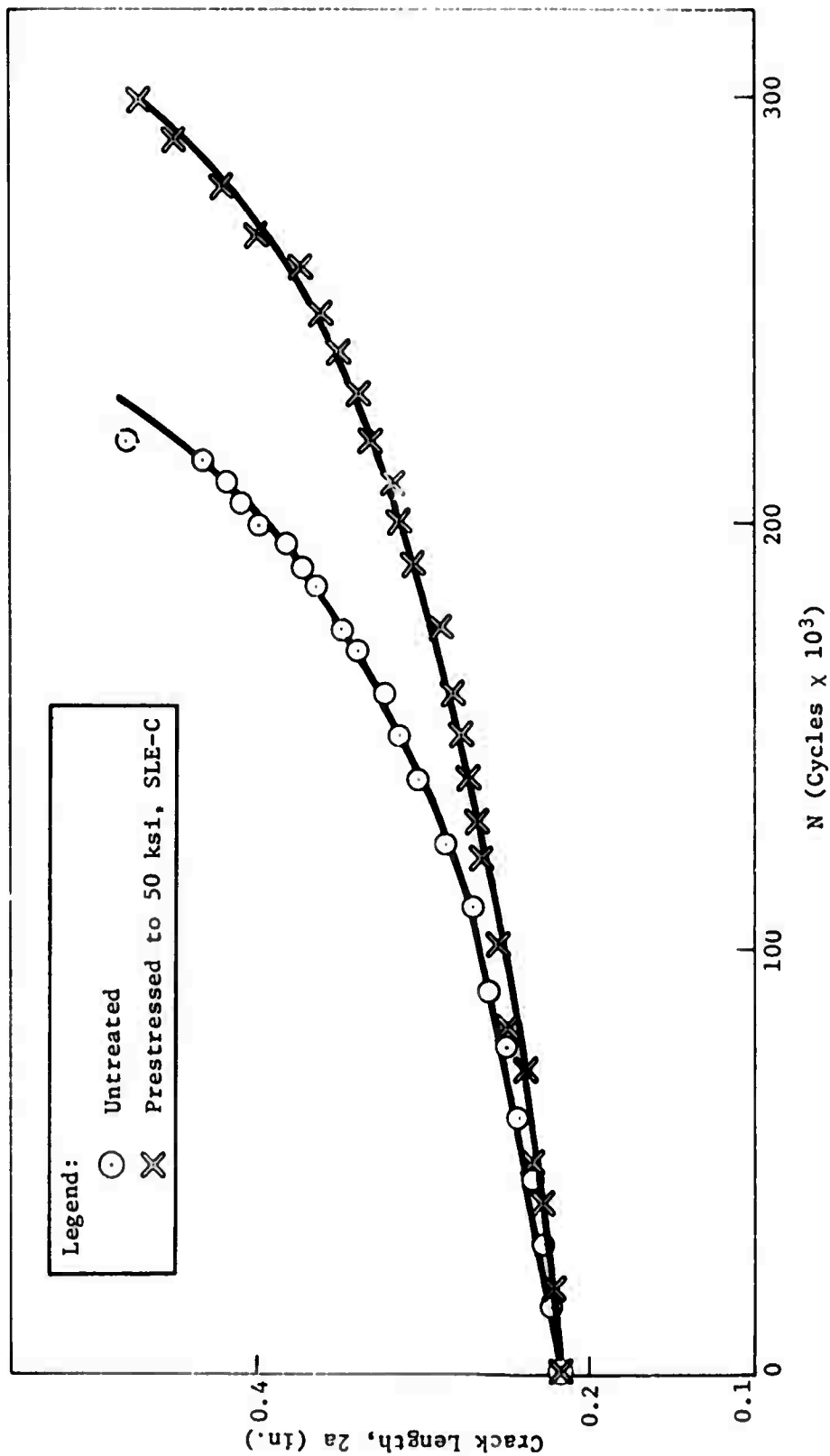


Figure IV-3 Fe-3% Si Cyclic Crack Propagation Behavior, Plane Stress Condition

25,000 psi. The initial crack length, $2a$, was 0.22 in. One specimen was untreated, the other prestressed to 50 ksi and 0.003 in. removed from each face. For the untreated specimen, the initial flow started to propagate after 297,000 cycles, whereas initial flow in the SLE-C specimen did not propagate up to 396,000 cycles. The crack length increased with cycling, and the rate of crack propagation, da/dN , increased with increasing crack length because ΔK was increasing, although applied stress, $\Delta\sigma$, remained unchanged. In Figure IV-3, a smooth curve through data points is drawn and the slope da/dN for any crack length, a , or the corresponding ΔK is calculated. In Figure 4, da/dN is plotted against ΔK . Note that specimens whose surface layer had been eliminated have better crack resistance. For instance, at a ΔK of 9.8 ksi in., the untreated specimen has a da/dN of 3.3×10^{-7} in./cycle, whereas the SLE-C treated specimen has a da/dN of 1.8×10^{-7} in/cycle. In other words, improvement by a factor of 1.8 is obtained. The improvement is a function of ΔK . At a ΔK of 12 ksi in. the improvement is by a factor of 1.2.

These results can be explained in terms of the surface-layer concept. As shown in Chapter I, the surface layer in Fe-3% Si alloy is a region of higher dislocation density. The dislocation density at the surface of Fe-3% Si strained 1% is $10^8/\text{cm}^2$, while beyond 100μ from the surface, the dislocation density is $5 \times 10^6/\text{cm}^2$. The chemical removal of 100μ of surface layer eliminates this layer. The surface layer presumably supports a pile-up of dislocations of one sign. The local stresses associated with the surface layer can exceed the fracture stress, as discussed in Chapter II. Thus, elimination of the surface layer results in a more crack-resistant material.

To verify these ideas, detailed metallographic observations were made in the region near the surface of the specimen in the vicinity of the crack.

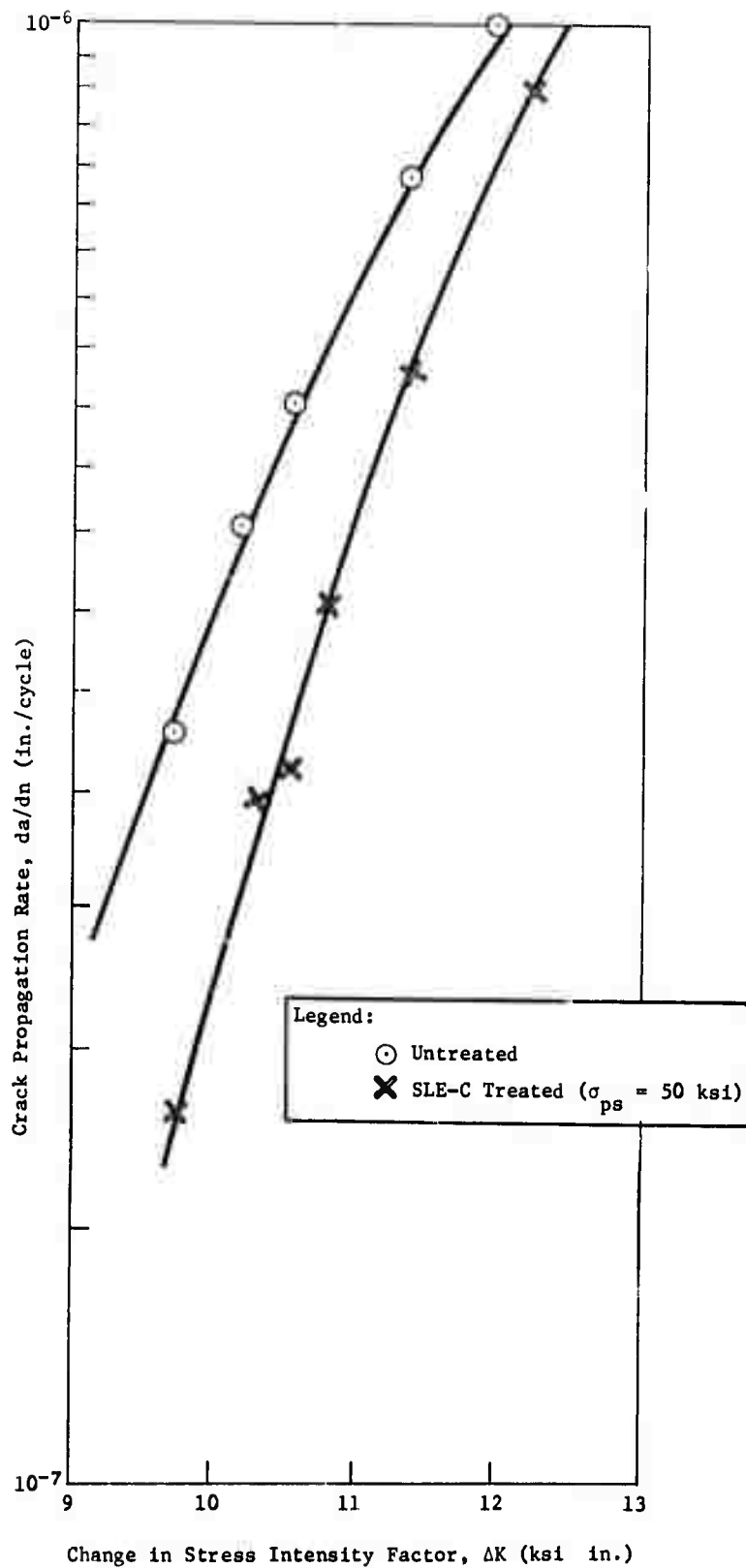
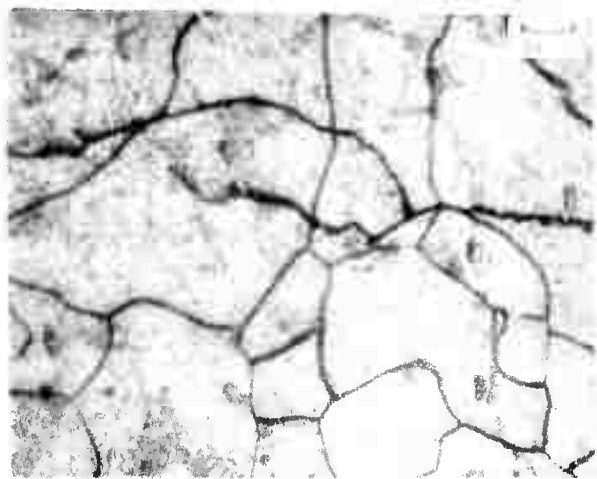


Figure IV-4 Fe-3% Si Crack Growth Rate Plane Stress Condition

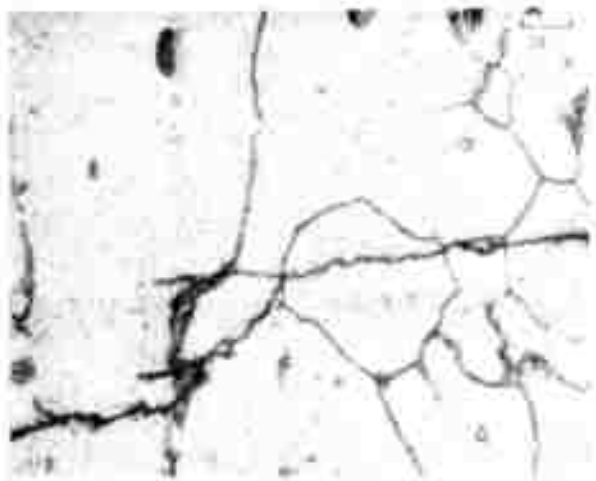
A section containing the crack was cut from the plane stress specimen after the crack had been propagated to a length, $2a$, of 0.4783 in. This section was given the ageing treatment as described in the experimental procedures section.

The specimen was then etched to reveal dislocation etch pits. Three sets of observations were made on the untreated and SLE-treated specimens. First a series of metallographic observations were made after removing 0.001 in. from the surface and etching the specimen. Then a further 0.002 in. was removed from the surface. The specimen was etched and observations of dislocation etch pits were made. Finally, 0.003 in. more was removed from the surface, the specimen re-etched and dislocation etch pits observed. A number of photographs were made and the typical ones are given in Figure IV-5 for the untreated and SLE-treated specimens. Note that the untreated specimen contains a greater dislocation density than the SLE-treated specimen in all cases. For the untreated specimens, dislocation density decreased with distance from the surface while, for SLE-treated specimens, dislocation density is essentially constant with depth. These observations imply that the initial condition of the surface layer governs the crack propagation rate.

It appears, in accordance with the results given in Chapter II, that the dislocation density must reach a given critical value for cracks to form. However, in the SLE case, because the initial dislocation density is low at the surface, it will require a large larger number of cycles of sufficient stress amplitude to generate the critical concentration necessary in crack formation and propagation. Although the dislocation density in the interior portions of the crack front is the same for the SLE-treated and untreated specimens, the initially low dislocation surface layer has a retarding effect on the overall crack growth rate.

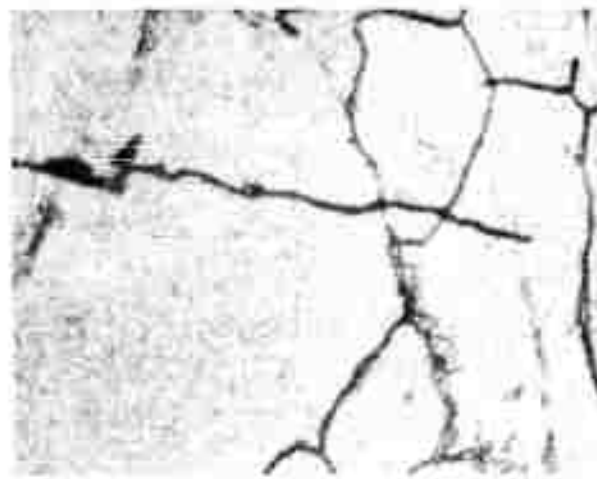


(a) $\Delta x = 0.001$ in.



(d) $\Delta x = 0.001$ in.

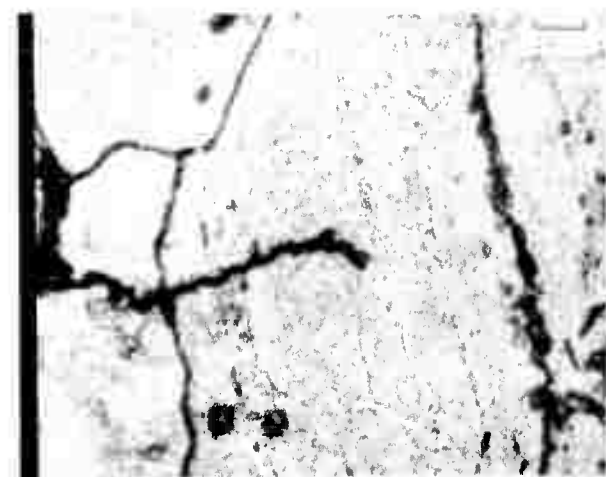
Reproduced from
best available copy.



(b) $\Delta x = 0.003$ in.



(e) $\Delta x = 0.003$ in.



(c) $\Delta x = 0.006$ in.



(f) $\Delta x = 0.006$ in.

Figure IV-5 Dislocation Density as a Function of Depth, Δx , in Vicinity of Crack in Untreated (a, b, c) and SLE-Treated (d, e, f) Fe-3% Si

REFERENCES

1. I.R. Kramer and A. Kumar: "The Effects of Surface Layer on Plastic Deformation and Crack Propagation". Semi Annual Report Contract DAAG 46-70-C-0102 August 1971.
2. I.R. Kramer and N. Balasubramanian: Enhancement of the Creep Resistance of Metals, to be published.
3. I.R. Kramer and A. Kumar: "The Influence of Environment and Surface Layer on Crack Propagation and Cyclic Behavior". Paper presented at Int. Conf. on Corrosion Fatigue, Storrs, Connecticut, June 14, 1971.
4. G.T. Hahn, P.N. Mincer and A.R. Rosenfield Exptl. Mech. 18 1 (1971).
5. G.T. Hahn, R.G. Hoagland and A.R. Rosenfield Met. Trans. 3 1189 (1972).
6. P. Lukes, M. Klesnil and R. Fiedler, Phil Mag. 13 799 (1970).
7. C. E. Morn, Metal Progress 56 696 (1949).

V. Deformation under Sustained Load

INTRODUCTION

We have measured (Ref 1) the rate of fatigue crack propagation in three materials--titanium (6Al-4V), aluminum 2014-T6, and 4130 steel--under plane stress and plane strain conditions. Data showed that crack resistance of these materials can be increased by a very simple treatment--prestressing the material to the proportional limit and then eliminating the surface layer formed as a result of this operation (S-SLE treatment). This elimination can be done by relaxing the surface-layer stress as a function of time for a sufficiently long period. In some cases, such as precipitation hardening alloys, dislocations in the surface layer are strongly pinned, and surface-layer stress does not seem to relax. For these materials, chem-milling about 0.005 in. from the surface removes the surface layer.

It is relatively easy to understand why this simple treatment improves the crack propagation resistance under cyclic loading conditions. Previous work showed that during cycling the surface-layer stress increased and, when it attained a critical value, fracture occurred. The details are given in Chapter II. However, it is not as simple to understand fracture under sustained loading. In this case, although the applied stress is substantially below the fracture strength, cracks will form with time, and fracture may occur. The limit stress that causes crack initiation is known to be strongly affected by environment. Thus, it would appear that, under sustained loading, dislocation rearrangement or multiplication must be occurring in local areas to produce a stress larger than the fracture stress. It is suspected that during this period the surface layer stress increases in local regions of the slip bands, and fracture occurs as a result of piled-up arrays.

This chapter describes an experimental investigation that

attempted to detect slip-line motion or formation under sustained loading. This was done to observe changes that might occur just before crack propagation. Therefore, metallographic changes as a function of time were followed at a given value of stress intensity factor. Both plane stress and plane strain specimens were used.

EXPERIMENTAL TECHNIQUES

The following tabulation shows the materials procured from vendors--

<u>Material</u>	<u>Thickness (in.)</u>	<u>Vendor</u>
Aluminum 2014-T6	0.125	Alcoa
	1.0	Kaiser

Specimen Preparation and Heat Treatment

The specimens were machined from sheet or plate stock in the as-received condition, then stress relief annealed to remove the residual stress machining. The aluminum specimens were heat treated at 250°F for 1 hr and furnace cooled. The aluminum blanks for specimens requiring SLE treatment were first prestressed to 54 ksi (just below the proportional limit of 56 ksi). Then specimens were machined from these blanks and the surface layer eliminated by chem-milling about 0.005 in. from the surface.

Specimen Configuration

Both plane stress and plane strain specimens were used. The specifications of ASTM's Committee E-24 were followed. According to this specification, minimum thickness for plane strain is $2.5 \left(\frac{K_{Ic}}{\sigma_y} \right)^2$ (Ref 2) where K_{Ic} is the plane strain fracture

toughness, and σ_y is the yield strength. In the case of 2014-T6, this minimum thickness turns out to be 1 in. For the plane strain case, compact tensile specimens (CTS) were used. The configurations of center-cracked specimens and CTS specimens are shown in Figures 1 and 2, respectively.

Testing

The prestressing was done in a Baldwin (50,000-lb) machine. Testing was done in a creep rack that had a lever arm ratio of 20 to 1. After the stress relief anneal, a 0.125-in.-diameter hole was drilled in the case of center-cracked specimens. A jeweler's saw was used to form the wings of the initial flaw. This provided the starter crack. This crack was sharpened by fatiguing at 20 Hz between stresses of 2500 and 10,000 psi. A total of 56,000 fatigue cycles brought the crack length up to 0.2233 in. A similar procedure was used for CTS specimens, i.e., fatigue-sharpened starter crack. The specimens were loaded to 90% of K_c for plane stress specimens, 32 ksi $\sqrt{\text{in.}}$ and 90% of K_{Ic} for plane strain specimens, 16 ksi $\sqrt{\text{in.}}$ Metallographic observations were made as a function of time.

Metallography

The specimens had been polished with 1- μ diamond paste before testing. After loading, replicas of the specimen surface near the crack front were taken as a function of time. The time sequence followed a geometric progression 1, 2, 4, 8 min, up to 500 hours. The surface was cleaned with acetone and replicated on a cellulose acetate tape 5 mil thick. In the case of plane strain specimens, the crack opening displacement (COD) was measured by scribing grid lines on the specimen on either side of the crack and observing

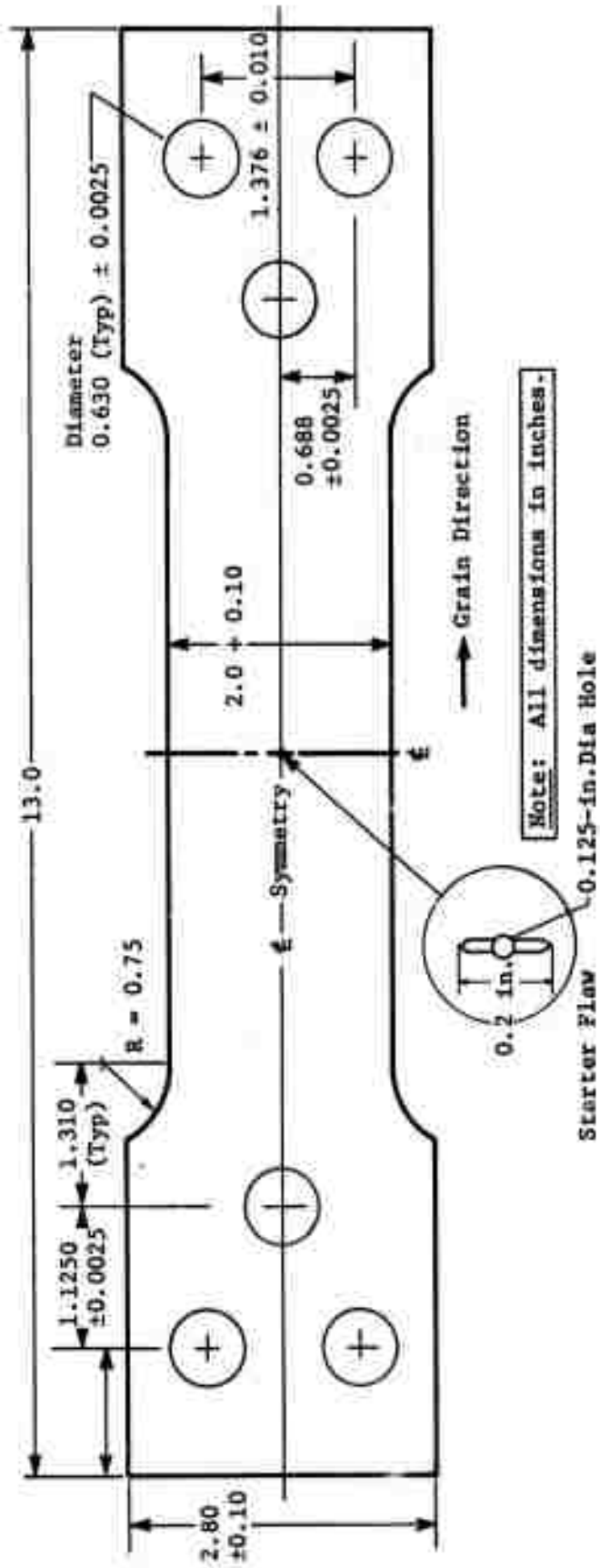
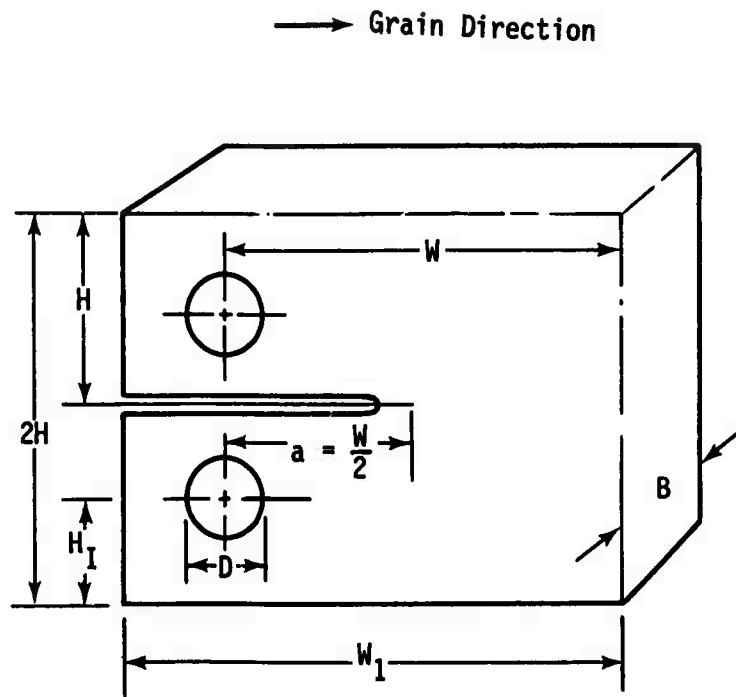


Figure V-1 Center-Cracked Specimen Configuration



$W = 2.0B$	$D = 0.5B$
$a = 1.0B$	$W_1 = 2.5B$
$H = 1.2B$	$H_1 = 0.65B$

Figure V-2 Proportions of Modified Compact Tension Specimen

them through a microscope at a magnification of 10X.

RESULTS AND DISCUSSION

Replicas were taken as a function of time at a constant value of stress intensity factor. The stress intensity factor was calculated as

$$K = \frac{L}{BW} \frac{5a}{F}$$

where L - load

W - width of specimen

B - thickness

a - crack length

$$F = W \tan \frac{\pi a}{W} \text{ for center-cracked specimens}$$

and $F = 23.12 - 67.67 \left(\frac{a}{W}\right) + 97.31 \left(\frac{a}{W}\right)^2$ for CTS specimens, following Wessel (Ref 3).

Experiments including center-cracked specimens were preliminary work. Hence, a range of K_c values of 25 ksi $\sqrt{\text{in.}}$ to 23 ksi $\sqrt{\text{in.}}$ was used (the K_c value). Based on these experiments, a K value that is 90% of K_c was arrived at as a convenient stress intensity factor at which the crack front could be studied as a function of time. The CTS specimen was loaded to a K value of 16 ksi $\sqrt{\text{in.}}$, which is 90% of K_{Ic} . A typical metallograph made from the replica is shown in Figure V-3. The magnification is 75X. Immediately on loading, crack branching was observed, as seen in Figure V-3. No further metallographic changes were observed as a function of time over a period of 500 hr; nor was there a change in crack opening displacement. These experiments were repeated at a K value 94% of K_{Ic} with substantially the same results. This suggests the possibility that metallographic changes as a function of time might be taking place elsewhere in the specimen rather than on the surface observed.



Figure V-3 Branch Crack Formed during Application of Load on CTS Specimen of 2014-T6, 75X

REFERENCES

1. I.R. Kramer and A. Kumar: "The Effects of Surface Layer on Plastic Deformation and Crack Propagation," Semi-annual Report, Contract DAAG46-70-C-0102, August 1971.
2. W.F. Brown, Jr. and J.E. Srawley in "Fracture Toughness Testing and Its Applications," ASTM STP 381, 1965.
3. E.T. Wessel: Eng. Frac. Mech, 1 (1968), 77.